Stromal regulation of vessel stability by MMP14 and TGFβ

Nor E. Sounni[1,*], Kerstin Dehne[1,*], Leon van Kempen[1,9], Mikala Egeblad[3,10], Nesrine I. Affara[2], Ileana Cuevas[4], Jane Wiesen[2], Simon Junankar[1], Lidiya Korets[2], Jake Lee[1], Jennifer Shen[1], Charlotte J. Morrison[6,7], Christopher M. Overall[6,7], Stephen M. Krane[6], Zena Werb[3,5], Nancy Boudreau[4,5] and Lisa M. Coussens[1,2,5,‡]

SUMMARY

Innate regulatory networks within organs maintain tissue homeostasis and facilitate rapid responses to damage. We identified a novel pathway regulating vessel stability in tissues that involves matrix metalloproteinase 14 (MMP14) and transforming growth factor beta 1 (TGFβ$_1$). Whereas plasma proteins rapidly extravasate out of vasculature in wild-type mice following acute damage, short-term treatment of mice in vivo with a broad-spectrum metalloproteinase inhibitor, neutralizing antibodies to TGFβ$_1$, or an activin-like kinase 5 (ALK5) inhibitor significantly enhanced vessel leakage. By contrast, in a mouse model of age-related dermal fibrosis, where MMP14 activity and TGFβ bioavailability are chronically elevated, or in mice that ectopically express TGFβ in the epidermis, cutaneous vessels are resistant to acute leakage. Characteristic responses to tissue damage are reinstated if the fibrotic mice are pretreated with metalloproteinase inhibitors or TGFβ signaling antagonists. Neoplastic tissues, however, are in a constant state of tissue damage and exhibit altered hemodynamics owing to hyperleaky angiogenic vasculature. In two distinct transgenic mouse tumor models, inhibition of ALK5 further enhanced vascular leakage into the interstitium and facilitated increased delivery of high molecular weight compounds into premalignant tissue and tumors. Taken together, these data define a central pathway involving MMP14 and TGFβ that mediates vessel stability and vascular response to tissue injury. Antagonists of this pathway could be therapeutically exploited to improve the delivery of therapeutics or molecular contrast agents into tissues where chronic damage or neoplastic disease limits their efficient delivery.

INTRODUCTION

When tissues are injured, vasodilation of capillaries and extravasation of plasma proteins into the interstitial tissue mark the onset of vascular remodeling following tissue assault (Bhushan et al., 2002). These processes are crucial not only for initiating a healing response, but also for enabling re-establishment of tissue homeostasis. Although molecules that regulate aspects of vascular stability and/or leakage have been identified, the molecular mechanisms controlling transport of macromolecules across the endothelium have only recently begun to be defined. Extravasation of plasma proteins is subject to regulation by many factors – some affect vessel leakiness by regulating the formation of openings in venular endothelium, resulting in exposure of subendothelial basement membranes to capillary lumens (Feng et al., 1997; Hashizume et al., 2000; Feng et al., 2002; McDonald and Baluk, 2002), whereas others regulate the diffusion of macromolecules into

[1]Cancer Research Institute, [2]Department of Pathology, [3]Department of Anatomy, [4]Department of Surgery, [5]Helen Diller Family Comprehensive Cancer Center, University of California, San Francisco, 513 Parnassus Ave., San Francisco, CA 94143, USA
[6]Department of Oral Biological and Medical Sciences, [7]Department of Biochemistry and Molecular Biology, University of British Columbia, Centre for Blood Research, Life Sciences Institute, 2350 Health Science Mall, Vancouver, British Columbia V6T 1Z3, Canada
[8]Department of Medicine, Harvard Medical School, Massachusetts General Hospital, CIID, 149 13th Street, Charlestown, MA 02129, USA
[9]Present address: Department of Pathology, Radboud University Nijmegen Medical Centre, 6500 HB Nijmegen, The Netherlands
[10]Present address: Cold Spring Harbor Laboratory, One Bungtown Rd, Cold Spring Harbor, NY 11724, USA
*These authors contributed equally to this work
‡Author for correspondence (Lisa.Coussens@ucsf.edu)

interstitium (McKee et al., 2001; Pluen et al., 2001; Brown et al., 2003). In the resting state, large plasma proteins such as albumin are transported across the endothelial body through a series of vesicles that may or may not fuse to form transcellular channels (Mehta and Malik, 2006), underscoring the fundamental importance of transcellular pathways in maintaining the semi-permeable nature of continuous endothelium (Drab et al., 2001). In contrast to this transcellular-type transport, the majority of plasma protein leakage in response to inflammatory stimuli occurs through the formation of gaps between cells, i.e. 'paracellular' leakage (Predescu et al., 2002; Mehta and Malik, 2006).

Vascular responses to tissue damage are accompanied by type I collagen remodeling in perivascular stroma (Page and Schroeder, 1982). The extracellular matrix (ECM), including fibrillar type I collagen, is rapidly remodeled around blood vessels following the acute inflammatory processes that accompany tissue damage, as well as during chronic vascular pathologies, e.g. atherosclerosis, hypertension, varicosis, restenosis, etc. (Jacob et al., 2001). Matrix metalloproteinases (MMPs) that cleave interstitial collagens also play a crucial role in regulating perivascular matrix remodeling. Indeed, sustained MMP activity is associated with some vascular pathologies, including atherosclerosis, hypertension restenosis and aneurysm (Mott and Werb, 2004; Page-McCaw et al., 2007). MMPs can further contribute to vascular remodeling by liberating vasoactive cytokines from stromal matrices, including the angiogenic/permeability factor vascular endothelial growth factor (VEGF) (Bergers et al., 2000; Sounni et al., 2002), as well as activating latent growth factors such as transforming growth factor β (TGFβ) (Yu and Stamenkovic, 2000; Mu et al., 2002; Wang et al., 2006). Despite extensive investigations into the roles of MMPs as mediators of chronic vascular pathologies, surprisingly little is

known regarding their role in acute vascular responses, or how they contribute to vascular homeostasis. Accordingly, we investigated whether MMPs participate in the early phases of acute tissue repair, and whether they contribute to the appropriate vascular responses to tissue damage. In this study, we identified a post-translational pathway whereby type I collagen fibrils regulate perivascular MMP activity and TGFβ bioavailability, which in turn regulate vascular homeostasis by altering vessel stability and leakage.

RESULTS

Loss of MMP14 activity increases steady-state vascular leakage

Previous studies have reported that ectopically applied collagenase, or a reduced accumulation of collagen fibrils in tissue, correlates with enhanced 'drug' delivery to tumors (McKee et al., 2001; Brown et al., 2003; Loeffler et al., 2006; Gade et al., 2009), thus indicating that the organization and structure of perivascular collagen fibrils regulate vascular leakage. To directly assess whether inhibition of collagenolytic MMP activity impacted vascular leakage, we used the Miles assay (Miles and Miles, 1952), which is an in vivo assay of vascular leakage, to analyze the acute cutaneous vascular response to mustard oil (MO) in mice that were pretreated systemically with the broad-spectrum metalloproteinase (MP) inhibitor GM6001. Wild-type (wt) mice were administered with GM6001 (or vehicle) for 5 days, followed by acute challenge with MO versus vehicle (mineral oil, MnO) (Inoue et al., 1997), one minute after receiving an intravenous (i.v.) injection of Evans Blue (EB) dye, which binds to and marks serum albumin. As expected, following MO exposure, EB extravasation rapidly increased in ear tissue interstitium, indicative of plasma protein leakage (Fig. 1A). Surprisingly, however, prior treatment with GM6001 significantly increased EB leakage (Fig. 1A). This indicated that the inhibition of steady-state MP activity rendered vessels more susceptible to MO-induced acute leakage, and implied a link between steady-state MP activity and vascular leakage.

To identify the MP associated with this response, we assessed steady-state and MO-induced EB leakage, using the Miles assay, in control and homozygous null mice lacking genes that encode collagenolytic MMPs, i.e. MMP2, MMP8, MMP13 and MMP14 (Fig. 1B,C). Steady-state and MO-induced vascular leakage characteristics in the ear skin were similar in MMP2, MMP8 and MMP13 null skin as compared with the skin from littermate control mice (Fig. 1B, and data not shown). However, in mice lacking MMP14, the steady-state vascular leakage of EB from ear skin was elevated compared with aged-matched controls (Fig. 1C), and similar to the leakage following MO exposure. The steady-state leakage of capillaries in back skin was also higher in MMP14 null mice versus age-matched heterozygous and wild-type littermates (Fig. 1D). Thus, the enhanced leakage of cutaneous vessels in mice lacking MMP14 indicates that MMP14 participates in regulating steady-state vascular leakage.

Perivascular collagen fibrils increase metalloproteinase activity and regulate vascular leakage

To further explore how collagen fibril organization and MMP14 activity impacted vascular leakage, we utilized a mouse model of age-related dermal fibrosis, Colα1(I)$^{r/r}$ mice (Liu et al., 1995), which exhibit threefold higher tissue collagenolytic activity in skin (Fig. 2A). The Colα1(I)$^{r/r}$ mice also exhibited a ~50% reduction in leakage following MO exposure (Fig. 2B), which could be rescued fully by
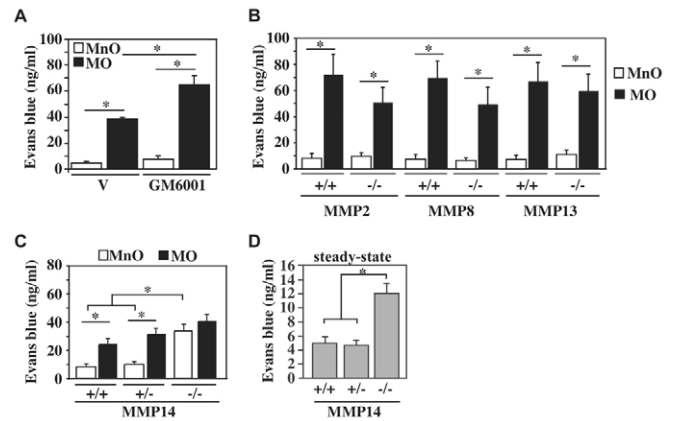

Fig. 1. MMP14 regulates vascular stability. (A) Quantitative assessment of Evans Blue (EB) dye leakage into interstitial tissue from the ears of control and GM6001-treated mice (four mice/experimental group) that were ectopically exposed to either mineral oil (MnO; white bars) or mustard oil (MO; black bars). Data reflect mean ± standard error of the mean (S.E.M.). *P<0.01. (B) Quantitative assessment of EB leakage into interstitial tissue from the ears of MMP2, MMP8 or MMP13 homozygous null (–/–) mice versus respective control (+/+) mice (four mice/group) treated with mineral oil or mustard oil. Data reflect mean ± S.E.M. *P<0.01. (C) Quantitative assessment of EB leakage into interstitial tissue from the ears of MMP14 homozygous null (–/–) mice versus aged-matched control wild-type or heterozygous (+/+ or +/–) mice (four mice/group) treated with mineral oil or mustard oil. Data reflect mean ± S.E.M. *P<0.01. (D) Quantitative assessment of EB leakage into the interstitial tissue of dorsal skin in untreated age-matched wild-type (+/+), MMP14$^{+/-}$ or MMP14$^{-/-}$ mice (four mice/experimental group). Data reflect mean ± S.E.M. *P<0.01.

prior treatment of mice with GM6001 (Fig. 2C). Although the levels of MMP14 protein are similar in wt and Colα1(I)$^{r/r}$ mice (Fig. 2D), we observed that MMP14 activity, as evidenced by activation of proMMP2, is markedly enhanced in an ex vivo bioassay using collagen from Colα1(I)$^{r/r}$ mice (Fig. 2E), and that this enhanced activity is reflected by constitutive activation of MMP2 in Colα1(I)$^{r/r}$ mice in vivo (Fig. 2F). To re-affirm that MMP2 was not directly responsible for the restricted vascular leakage in Colα1(I)$^{r/r)}$ mice, selective loss of MMP2 in Colα1(I)$^{r/r}$MMP2$^{-/-}$ mice (Egeblad et al., 2007) did not alter Colα1(I)$^{r/r}$ susceptibility to MO-induced capillary leakage (Fig. 2G).

Metalloproteinase-mediated resistance to vascular leakage is accompanied by decreased appearance of leakage sites in vessels with perivascular cell coverage

Colα1(I)$^{r/r}$ mice were also found to be resistant to acute vascular leakage induced by either serotonin or VEGF (Fig. 3A). Moreover, the resistance to VEGF leakage in Colα1(I)$^{r/r}$ mice was not linked to changes in the expression or activation of VEGF receptor 2 (VEGFR2) (Fig. 3B), and together suggest that the elevated collagenolytic activity in Colα1(I)$^{r/r}$ mice reduces the acute vascular leakage induced by a variety of stimulants.

To further evaluate the pathologic basis underlying reduced vascular leakage in Colα1(I)$^{r/r}$ mice, we assessed the organization, architecture and diameter of cutaneous capillary networks in ears from Colα1(I)$^{r/r}$ mice and their control littermates following MO exposure. We assessed capillary beds by fluorescent angiography
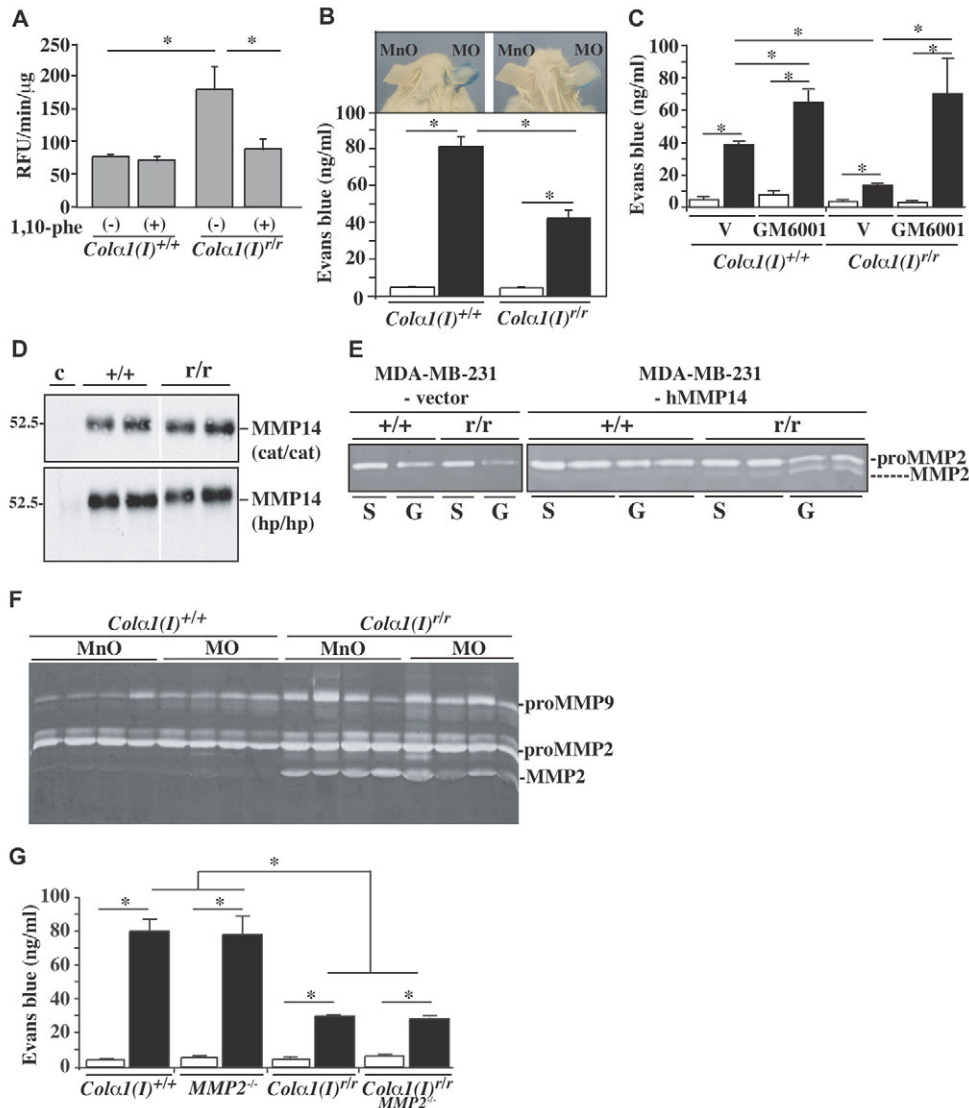
Fig. 2. Increased MMP14 activity is associated with restricted vascular leakage. (A) Total MP activity (relative fluorescence units, RFU) in ear tissue lysates from Colα1(I)$^{+/+}$ and Colα1(I)$^{r/r}$ mice (four mice/experimental group), as assessed by a fluorogenic solution assay utilizing quenched DQ-gelatin. Incubation of lysates with 1,10-phenanthroline (+; 4.0 μM) eliminated cleavage of the fluorogenic substrate. Data reflect mean ± S.E.M. *P <0.01. (B) Upper panels document EB dye leakage (blue staining) in the ears of Colα1(I)$^{+/+}$ (left) and Colα1(I)$^{r/r}$ (right) mice following application of mineral oil (MnO; left ear) or mustard oil (MO; right ear). The lower panel shows a quantitative assessment of EB leakage into interstitial tissue from Colα1(I)$^{+/+}$ and Colα1(I)$^{r/r}$ mice (five mice per experimental group) treated with mineral oil (white bars) and mustard oil (black bars). Data reflect mean ± S.E.M. *P=0.0001. (C) Treatment of Colα1(I)$^{+/+}$ and Colα1(I)$^{r/r}$ mice (five mice/experimental group) for 5 days with GM6001 versus vehicle (V) renders Colα1(I)$^{+/+}$ mice hypersensitive to the vascular leakage induced by mustard oil (black bars), as compared with mineral oil (white bars), and restores the acute vascular responses in Colα1(I)$^{r/r}$ mice to wt levels. Data reflect mean ± S.E.M. *P<0.02. (D) Western blot of immunoprecipitated MMP14 protein from the skin of wild-type (+/+) and Colα1(I)$^{r/r}$ (r/r) mice. Upper panel shows MMP14 immunoprecipitated and blotted with antibodies against the catalytic (cat/cat) domain, and the lower panel shows MMP14 recovered and probed with antibodies against the hemopexin (hp/hp) domain. The left lane ('c') is a control lane, which lacked tissue lysates throughout the procedure. Molecular mass standards in kDa are shown to the left of the blot. (E) Gelatin zymography, representing MDA-MB-231 cells that were stably transfected with vector or full-length human *MMP14* cDNA, grown in gels comprised of collagen that was purified from either Colα1(I)$^{+/+}$ (+/+) or Colα1(I)$^{r/r}$ (r/r) mice. The cells were assessed for their ability to activate proMMP2 in either the gel (G) or supernatant (S) fractions. Cleared regions of gel indicating the presence of proMMP2 or MMP2 are shown. (F) Gelatin substrate zymography of tissue lysates from Colα1(I)$^{+/+}$ and Colα1(I)$^{r/r}$ mouse ears, topically treated with MnO or MO. The presence of cleared regions in the gel (white areas) representing proMMP9, proMMP2 and MMP2 are indicated, where each lane reflects lysates from one mouse. (G) Quantitative assessment of EB leakage in the ear skin of wild-type Colα1(I)$^{+/+}$, MMP2$^{-/-}$, Colα1(I)$^{r/r}$ and Colα1(I)$^{r/r}$/MMP2$^{-/-}$ mice (four mice/experimental group) in response to mustard oil (black bars), as compared with mineral oil (white bars). Data reflect mean ± S.E.M. *P<0.005.

using fluorescein-labeled *Lycopersicon esculentum* (tomato) lectin that specifically binds to the luminal surfaces of vascular endothelium (Thurston et al., 1996). The organization and diameter

of capillaries in quiescent vascular beds of control and Colα1(I)$^{r/r}$ mice were similar, both qualitatively (Fig. 3C) and quantitatively (Fig. 3D). However, following MO treatment, the total vessel area,
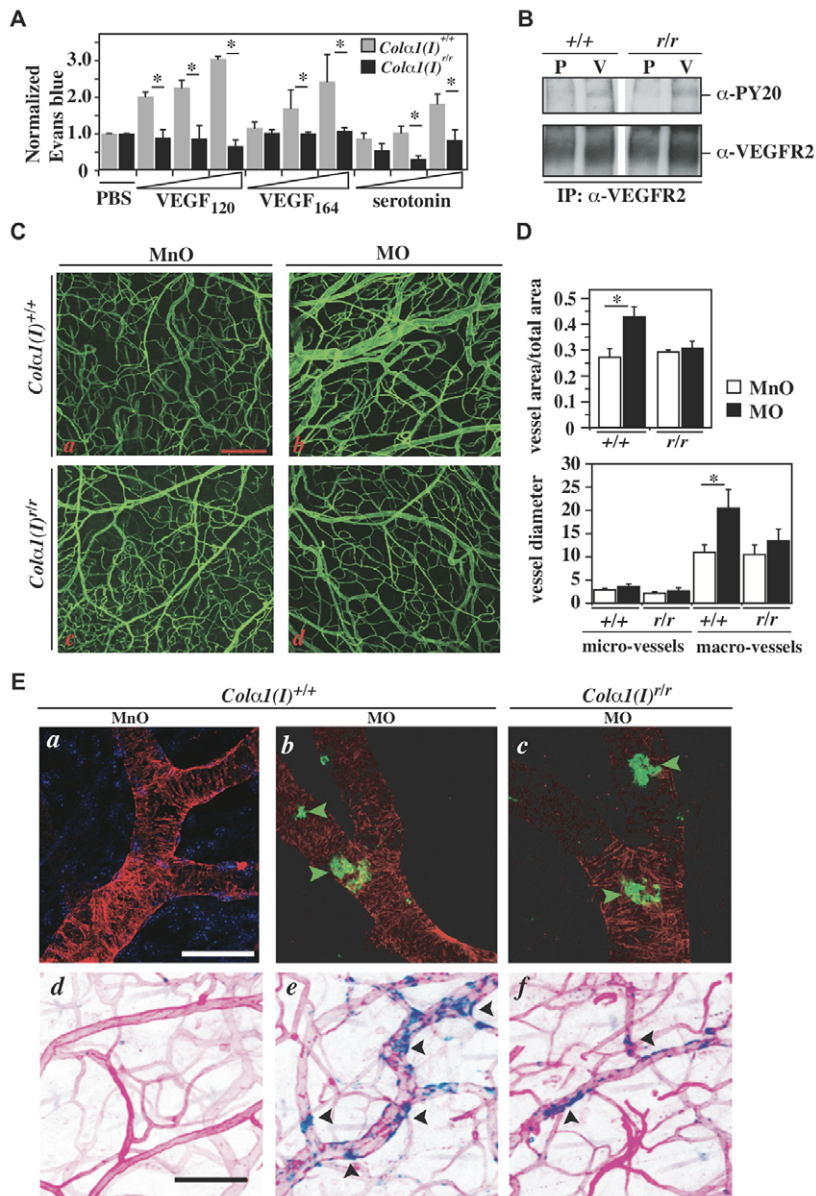
Fig. 3. Morphological assessment of vascular resistance to mustard oil. (A) Quantitation of EB leakage into interstitial stroma following intradermal (i.d.) injection of VEGF$_{120}$, VEGF$_{164}$ or serotonin in Colα1(I)$^{+/+}$ (grey bars) and Colα1(I)$^{r/r}$ (black bars) mice. *$P<0.05$ (two-tailed Mann-Whitney test) comparing Colα1(I)$^{+/+}$ mice with Colα1(I)$^{r/r}$ mice for the respective compounds at increasing doses. (B) Western blot analysis of phosphoVEGFR2 protein from tissue lysates (back skin) harvested from Colα1(I)$^{+/+}$ (+/+) or Colα1(I)$^{r/r}$ (r/r) mice (four mice/experimental group) following i.d. injection of VEGF$_{164}$ and immunoprecipitation with antibodies against VEGFR2. The lower panel shows the total VEGFR2 recovered from wt (+/+) or Colα1(I)$^{r/r}$ (r/r) mice. Blots were stripped and reprobed with antibodies against phosphotyrosine (PY20), shown in the upper panel. P, PBS; V, VEGF$_{164}$. (C) Fluorescent angiography of whole-mounted ears following fluorescein-labeled *Lycopersicon esculentum* lectin perfusion (green staining) of Colα1(I)$^{+/+}$ (panels *a,b*) and Colα1(I)$^{r/r}$ (panels *c,d*) mice treated with either mineral oil (MnO) or mustard oil (MO). Bar, 200 μm. (D) The upper graph shows a quantitative assessment of vascular area in the ears of Colα1(I)$^{+/+}$ (+/+) versus Colα1(I)$^{r/r}$ (r/r) mice (five mice/experimental group, S.E.M.) following mineral oil (white bars) or mustard oil (black bars) treatment. *$P=0.0357$. The lower graph shows a quantitative assessment of micro (<5 μm) and macro (>5 μm) vessel diameters in Colα1(I)$^{+/+}$ (+/+) and Colα1(I)$^{r/r}$ (r/r) ear skin (five mice/experimental group) following mineral oil (white bars) and mustard oil (black bars) treatment. Data reflect mean ± S.E.M. *$P=0.0001$. (E) Representative confocal images showing the perivascular cell phenotype and sites of vascular leakage. Panels *a-c*: immunohistochemical detection of αSMA-positive perivascular cells (red staining) in whole-mounted ears from Colα1(I)$^{+/+}$ (panels *a,b*) and Colα1(I)$^{r/r}$ (panel *c*) mice following mineral oil (panel *a*) or mustard oil (panels *b,c*) stimulation and intravenous (i.v.) injection of fluorescein-labeled *Ricinus communis* agglutinin I (green staining, arrowheads). Panels *d-f*: representative pseudocolored confocal images showing ears from Colα1(I)$^{+/+}$ (panels *d,e*) and Colα1(I)$^{r/r}$ (panel *f*) mice, where ears were treated with mineral oil (panel *d*) or mustard oil (panels *e,f*), followed by fluorescent angiography with fluorescein-labeled *Lycopersicon esculentum* lectin perfusion (pink staining; panels *d-f*) and rhodamine-labeled *Ricinus communis* agglutinin I (blue staining, arrowheads, panels *e,f*). The blue staining in panel *a* reflects DAPI staining of nuclei in the ear tissue. Bars, 200 μm (E, panels *a-c*); 100 μm (E, panels *d-f*).

and in particular the vessel diameter, increased significantly in control mice but remained unchanged in the skin of Colα1(I)$^{r/r}$ mice (Fig. 3C,D).

Since mural cell coverage of blood vessels contributes to vasodilation and extravasation of plasma proteins, we examined the presence of perivascular cells on venules in the skin from wt and Colα1(I)$^{r/r}$ mice by whole-mount immunodetection of α-smooth muscle actin (αSMA), a marker for mature perivascular cells (Verbeek et al., 1994). Interestingly, the position and morphology of αSMA-positive perivascular cells in vehicle-treated control versus MO-treated Colα1(I)$^{r/r}$ skin were indistinguishable (Fig. 3E, panels *a-c*).

Extravasation of plasma proteins into tissue interstitia is also regulated by the frequency of openings in venular endothelium (McDonald and Baluk, 2002); accordingly, we injected control and Colα1(I)$^{r/r}$ mice with fluorescein-labeled *Lycopersicon esculentum*

lectin (to visualize vasculature), in combination with rhodamine-labeled *Ricinus communis* agglutinin I (to visualize luminal openings). Following MO exposure, numerous leakage sites appeared in capillary beds of tissue from control mice (Fig. 3E, panel *e*), specifically in capillaries where perivascular cell coverage was prominent (Fig. 3E, panel *b*). However, the leakage sites were less abundant in MO-treated Colα1(I)$^{r/r}$ capillaries (Fig. 3E, panel *f*), indicating that the enhanced stability of vessels in Colα1(I)$^{r/r}$ mice correlated with reduced vasodilation following MO challenge and a diminished frequency of venular openings, independent of similar perivascular cell coverage.

MMP14 regulates TGFβ bioactivity and vascular stability

In addition to activating proMMP2, MMP14 also regulates the bioavailability of several chemokines and growth factors, most notably latent TGFβ (Werb, 1997; Mu et al., 2002; Alfranca et al.,

2008), which can profoundly impact vascular integrity. Given that MMP2 deficiency failed to alter vascular stability alone (Fig. 1B), or in combination with the Colα1(I)$^{r/r}$ mutation (Fig. 2G), we evaluated whether TGFβ$_1$ might mediate a MMP14- or collagen-regulated vascular response. We assessed whole-skin lysates by ELISA and found decreased levels of total TGFβ$_1$ in hyperleaky MMP14-deficient mice (Fig. 4A). We also found, in leakage-resistant Colα1(I)$^{r/r}$ mice, an elevated level of total TGFβ$_1$ that was independent of MMP2 (Fig. 4B and supplementary material Fig. S1A). Moreover, although *Tgfb1* mRNA expression (Fig. 4C) and the synthesis of latent TGFβ [the TGFβ latency-associated peptide (LAP)] (Fig. 4D) were similar in both wild-type and Colα1(I)$^{r/r}$ mice, we observed an increase in the mature, bioactive form of TGFβ$_1$ in Colα1(I)$^{r/r}$ tissue lysates (Fig. 4E,F), which was sensitive to GM6001 inhibition (Fig. 4G). Using an organotypic cell-based assay with cells that constitutively express MMP14, which were cultured on collagen derived from Colα1(I)$^{r/r}$ mice, we confirmed that the enhanced bioavailability of TGFβ$_1$ (and MMP2 activity) was indeed regulated directly by MMP14, and enhanced in the presence of mutant collagen fibrils (Fig. 4H and supplementary material Fig. S1B).

To directly demonstrate the role of TGFβ in regulating vascular stability and response, we administered a pan-TGFβ-neutralizing antibody, which neutralizes the bioactivity of all TGFβ isoforms in vivo (Yamamoto et al., 1999; Neptune et al., 2003), to 6-week-old control and Colα1(I)$^{r/r}$ mice prior to MO challenge. Similar to our results following the administration of GM6001 (Fig. 2C), neutralization of TGFβ in Colα1(I)$^{r/r}$ mice following MO stimulation resulted in appropriate acute vascular remodeling and reinstated the characteristic EB leakage to a level comparable to untreated controls (Fig. 4I).

The TGFβ type I receptor ALK5 (activin-like kinase 5) is expressed in both CD31$^+$ endothelial cells and αSMA-positive perivascular cells (data not shown). Similar to treatment with the pan-TGFβ-neutralizing antibody, responsiveness to MO-induced vascular leakage was restored following administration of an inhibitor of ALK5 (ALK5-I) (Fig. 4J); it also significantly enhanced the steady-state vascular leakage in unstimulated skin (Fig. 4K). Thus, consistent with the hyperleaky phenotype of MMP14 null mice, which have decreased steady-state levels of TGFβ, vessel stability and vascular leakage in Colα1(I)$^{r/r}$ mice are susceptible to regulation by modulation of metalloproteinase activity, TGFβ bioavailability and signaling downstream of ALK5.

Ectopic expression of TGFβ reduces acute vascular leakage

We reasoned that if neutralization of TGFβ or blockade of ALK5 signaling enhanced steady-state and acute leakiness, then sustained, ectopic expression of TGFβ$_1$ would phenocopy the elevated MMP14 activity that we observed in Colα1(I)$^{r/r}$ mice, and result in resistance to leakage. To test this hypothesis, we utilized an inducible TGFβ$_1$ bigenic mouse model (Cao et al., 2002) that expresses TGFβ$_1$ in basal keratinocytes of skin following induction by RU486 (Lu et al., 2004). Because exposure to RU486 for 6 days induced a psoriatic phenotype (Fig. 5A, panels *a,b*), we performed the EB leakage assay after 3 days of exposure to RU486, prior to the onset of psoriasis, when the skin of the bigenic mice appeared 'normal' (Fig. 5A, panel *a*) even though RU486-induced expression of TGFβ$_1$ was prominent in keratinocytes (Fig. 5A, panel *c*).

Significantly, the bigenic mice treated with RU486 for 3 days were resistant to MO-induced EB leakage (Fig. 5B), confirming that sustained ectopic expression of TGFβ phenocopied the vascular effects linked to elevated MMP14 activity in Colα1(I)$^{r/r}$ mice.

TGFβ attenuates vascular leakage in aged and neoplastic tissue

The data above indicate that MMP14-activated TGFβ$_1$ regulates vascular homeostasis and the vascular response to acute tissue damage via signaling through ALK5. To determine whether this signaling pathway was susceptible to regulation in aged tissues where fibrosis and the cross-linking of collagen fibrils can compromise tissue hemodynamics, we utilized aged C57BL/6 mice. Similar to young animals, transient blockade of ALK5 in aged mice led to enhanced vessel leakiness following MO stimulation (Fig. 6A).

To determine whether the ALK5 signaling pathway was also active in chronically leaky angiogenic vessels, such as those found in neoplastic tissues, we utilized two transgenic models of epithelial carcinogenesis (Guy et al., 1992; Coussens et al., 1996). Angiogenic blood vessels in the premalignant skin of K14-HPV16 transgenic mice exhibit increased steady-state leakiness (Eichten et al., 2007) in capillaries that are largely devoid of αSMA-positive perivascular cells (Fig. 6B,C). Transient ALK5 blockade in K14-HPV16 transgenic mice further increased vessel leakage and extravasation of EB dye (Fig. 6C). Together, these data indicate that the ALK5 signaling pathway remains susceptible to therapeutic modulation in both aged and angiogenic vessels.

Based on this, we hypothesized that antagonizing ALK5-mediated signaling in tumor vessels would enhance leakage and potentially improve the delivery of high molecular weight compounds, such as antibodies, liposomes or contrast agents, into the tumor interstitium. Moreover, to ensure that inhibition of TGFβ was influencing vascular permeability and not simply modulating bulk flow, we performed live imaging of mice to dynamically follow the leakage of high and low molecular weight dextrans into mammary carcinomas in MMTV-PyMT transgenic mice (Guy et al., 1992). ALK5 inhibition conferred a significant increase in the leakage of 70 kDa dextran into late-stage carcinomas (Fig. 6D,E). Moreover, although ALK5 blockade had no effect on the initial leakage of 10 kDa dextran, it significantly increased the retention of dextran in the tumor. Thus, transient blockade of ALK5 in live mice bearing large invasive tumors enhanced the leakiness of angiogenic vessels, enabling increased delivery of high molecular weight compounds and increased retention of low molecular weight compounds to tumor tissue. Together, these data indicate that TGFβ-mediated signaling through the ALK5 receptor in vascular cells regulates vascular stability and leakage in homeostatic, acutely damaged, aged, and angiogenic tissue, and thus reveals a therapeutic opportunity to enhance the delivery of drugs to tissue where hemodynamics limit that possibility.

DISCUSSION

Herein we describe a novel mechanism by which TGFβ regulates vessel stability and leakage in homeostatic, acutely damaged and angiogenic blood vessels. Our findings demonstrate that, in cutaneous vasculature, steady-state levels of MMP14 and TGFβ regulate homeostatic vascular leakage via ALK5 signaling, and that, together, they regulate extravasation of plasma proteins into the
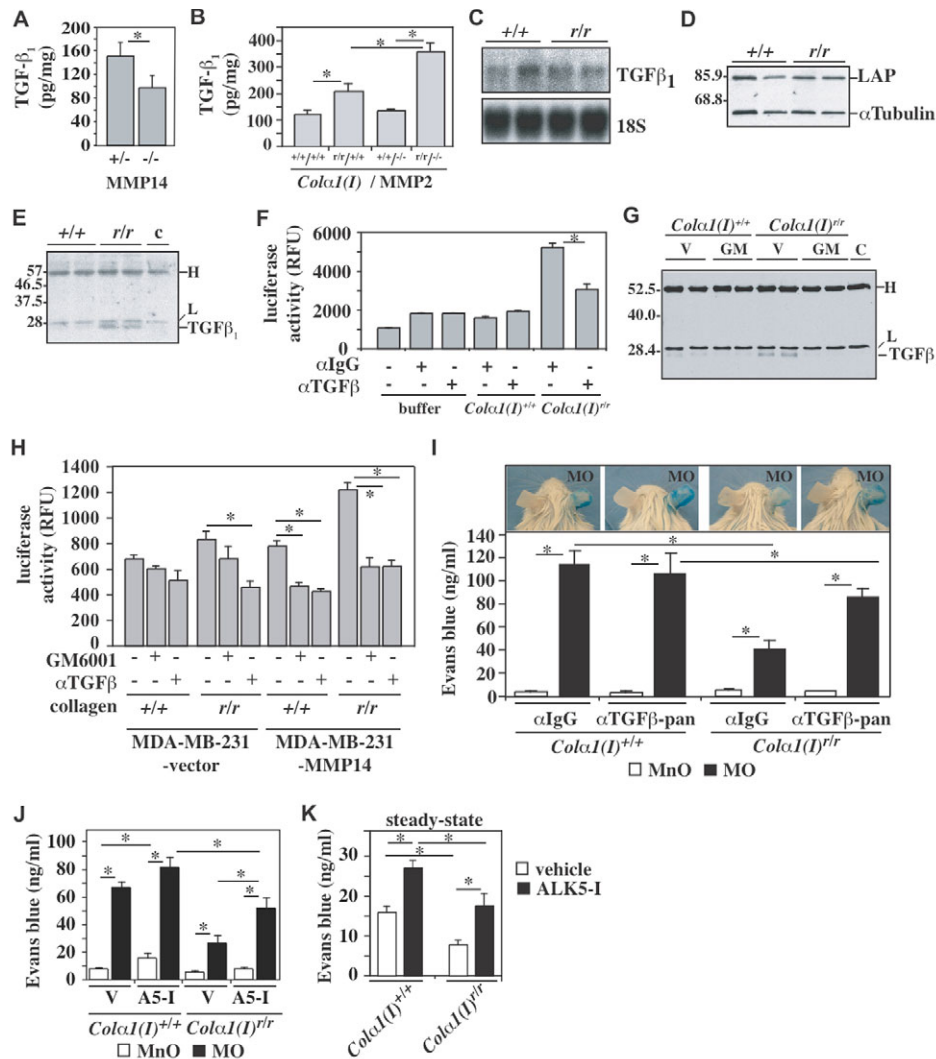
Fig. 4. MMP14-activated TGFβ restricts the vascular response. (A) ELISA of ear tissue lysates from control (MMP14^{+/−}) or MMP14 null (−/−) mice (three mice/experimental group), showing the reduced levels of total TGFβ1 in the skin of MMP14 null mice. Data reflect mean ± S.E.M. *P=0.0001. (B) Total TGFβ1 present in tissue lysates from wild-type ([+/+]/[+/+]), Colα1(I)[r/r] ([r/r]/[+/+]), MMP2^{−/−} ([+/+]/[−/−]) and Colα1(I)[r/r]/MMP2^{−/−} ([r/r]/[−/−]) ear skin (five mice/experimental group) measured by ELISA. Data reflect mean ± S.E.M. *P<0.01. (C) TGFβ1 mRNA in the ear skin from Colα1(I)[+/+] (+/+) and Colα1(I)[r/r] (r/r) mice, as assessed by northern blot analysis. The 18S RNA is shown as a control. (D) Western blot analysis of Colα1(I)[+/+] (+/+) and Colα1(I)[r/r] (r/r) ear tissue lysates under reducing conditions using an antibody to LAP. The ~75 kDa reactive band, corresponding to monomeric LAP, was identified by comparing it with α-tubulin (loading control). Molecular mass standards are given in kDa on the left. (E) Western blot analysis of immunoprecipitated proteins reveals the presence of an ~25 kDa reactive band, correlating to the mature bioavailable form of dimeric TGFβ1, in ear tissue lysates from Colα1(I)[r/r] (r/r) mice that is not detectable in tissue lysates from Colα1(I)[+/+] (+/+) mice. The lane labeled 'c' shows immune complexes in the buffer control (no tissue lysate). The presence of murine heavy (H) and light (L) immunoglobulin chains is also shown. (F) TGFβ1 bioavailability as assessed by PAI-1 luciferase reporter activity following incubation of MLE-PAI-1 cells with ear tissue lysates from Colα1(I)[+/+] or Colα1(I)[r/r] mice (lysates from four mice/experimental group, repeated in triplicate). Samples were incubated with anti-IgG control antibodies (αIgG) or pan-neutralizing antibodies against TGFβ (αTGFβ). Data reflect mean ± S.E.M. *P=0.01. (G) The presence of a low molecular weight ~25 kDa reactive band, correlating to the mature bioavailable form of dimeric TGFβ1, in ear tissue lysates from Colα1(I)[+/+] and Colα1(I)[r/r] mice is reduced by prior in vivo treatment of mice with GM6001(GM). The lane labeled 'c' shows immune complexes in the buffer control (no tissue lysate). The presence of murine heavy (H) and light (L) immunoglobulin chains is also shown. Molecular mass standards are given in kDa on the left. (H) Endogenous TGFβ1 bioavailability assessed by the PAI-1 luciferase reporter activity of MLE-PAI-1 cells, following incubation with supernatants harvested from MDA-MB-231 cells that were stably transfected with either vector or human MMP14 and grown in gels comprised of collagen purified from Colα1(I)[+/+] (+/+) or Colα1(I)[r/r] (r/r) mice. Supernatants were also treated with GM6001 or a pan-neutralizing antibody against TGFβ. Each data point reflects the mean ± S.E.M. from the supernatants of four wells, pooled and repeated in triplicate. *P<0.01. (I) Upper panels show EB leakage in the ears of Colα1(I)[+/+] (left two panels) and Colα1(I)[r/r] (right two panels) mice that were treated with non-specific immunoglobulin or neutralizing antibodies to all TGFβ isoforms, followed by topical exposure to mineral oil (left ear) or mustard oil (MO; right ear), with quantitation of leakage assessed using the Miles assay (five mice/experimental group). Data reflect mean ± S.E.M. *P<0.05. (J) Quantitative assessment of EB leakage in the interstitial ear tissue of Colα1(I)[+/+] and Colα1(I)[r/r] mice that were treated with mineral oil (MnO; white bars) and mustard oil (MO; black bars); the assessment was carried out after a 5-day pretreatment with vehicle (V) or an inhibitor to ALK-5 (A5-I). Each bar reflects five mice/experimental group and the data indicate mean ± S.E.M. *P<0.03. (K) Quantitative assessment of EB leakage in steady-state (unstimulated) Colα1(I)[+/+] and Colα1(I)[r/r] mice (back skin), assessed after treatment with vehicle (v) or ALK5 inhibitor (ALK5-I) for 5 days (four mice/experimental group). Data reflect mean ± S.E.M. *P<0.02.
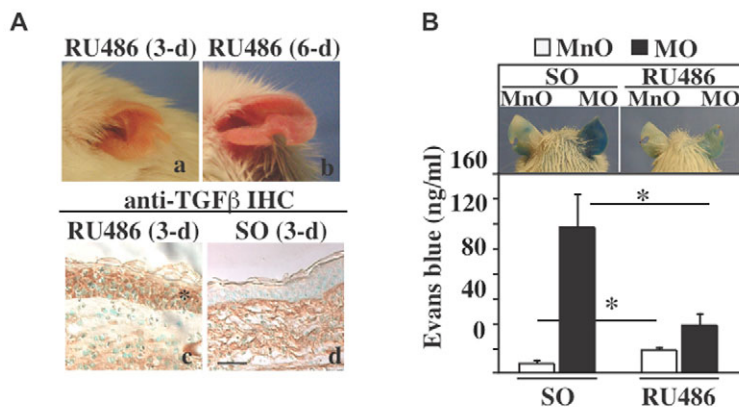
Fig. 5. TGFβ regulates steady-state and acute vascular leakage.
(A) Images of ears from bigenic K14-GLp65/tata.TGFβ₁ mice treated with RU486 on the ear skin for 3 days (a) or 6 days (b). Although ears exhibited psoriasis after 6 days of RU486-induced TGFβ₁ expression, ears appeared normal at 3 days. Lower panels show prominent TGFβ₁ immunoreactivity (*) in the ear skin of mice treated for 3 days with RU486 (c), but not for sesame oil (SO)-treated control mice (d). Bar, 50 μm (c,d). (B) Upper panels show the appearance of extravasated EB dye (blue staining) in the ears of bigenic K14-GLp65/tata.TGFβ₁ mice treated with mineral oil (MnO) or mustard oil (MO) after 3 days of pretreatment with sesame oil (SO) or RU486. The lower panel shows the corresponding quantitative analysis of EB dye leakage for each experimental condition (five mice/experimental group), as determined by the Miles assay. Data reflect mean ± S.E.M. *$P<0.01$.

tissue interstitium. Moreover, we provide further evidence that a post-translational pathway, mediated by perivascular type I collagen and MMP14 activity, controls the bioavailability of TGFβ. Taken together, these data indicate a central role for stromal metalloproteinase-activated TGFβ in mediating vascular homeostasis and remodeling, and further indicate that TGFβ and/or MMP14-selective antagonists may enhance vascular leakage and the delivery of therapeutics to tissues where hemodynamics limit efficient drug delivery (Fig. 7).

TGFβ regulates vascular homeostasis and the response to tissue damage
TGFβ has long been implicated as a regulator of vascular integrity (Pepper, 1997; Gleizes and Rifkin, 1999; Tuxhorn et al., 2002); vasculogenic and angiogenic processes (Dickson et al., 1995; Pepper, 1997); and endothelial and perivascular cell proliferation and/or differentiation (Sato, 1995; Yan and Sage, 1998; Vinals and Pouyssegur, 2001). Vascular abnormalities have also been described in TGFβ null mice, as well as in mice lacking various TGFβ type I and II receptors (Dickson et al., 1995; Seki et al., 2003; Seki et al., 2006). Despite extensive research on the impact of TGFβ on vasculature, the mechanisms by which TGFβ regulates vascular development and function are complex and remain controversial.

TGFβ differentially impacts endothelial and vascular smooth muscle cells in a concentration-, substrate- and tissue-specific context (Madri et al., 1992; Yan and Sage, 1998). For example, in bleomycin-induced pulmonary edema, TGFβ promotes vascular leakage by acting directly on pulmonary endothelial cells in concert with integrin α5β1 (Pittet et al., 2001; Su et al., 2007). TGFβ also induces the expression of angiopoietin-like protein 4 (Angpt-4) that, in turn, disrupts endothelial cell junctions, increases leakage, and promotes tumor cell emigration and metastasis to the lungs (Padua et al., 2008).

By contrast, in pancreatic tumors, vascular leakage is induced when TGFβ type I receptors are inhibited, accompanied by decreased Smad2-regulated signaling cascades, specifically in endothelia (Kano et al., 2007). In the brain, the inhibition of TGFβ type I ALK5 receptors also increases leakage (of the blood brain barrier), accompanied by changes in the expression of tight junction adhesion proteins (Ronaldson et al., 2009).

Our data indicate that, in cutaneous and mammary vessels, TGFβ acts primarily through the ALK5 receptor to restrict vessel leakage. Indeed, our localization data showing ALK5 expression in perivascular support cells (data not shown) concur with recent in vivo studies showing that the deletion of ALK5 in mice results in the loss of mural cells, whereas vessel lumens remain intact (Seki et al., 2006). Although we cannot rule out the possibility that TGFβ may also directly or indirectly influence the endothelial component of the vascular wall in vivo (Cambier et al., 2005; Roviezzo et al., 2005; Parikh et al., 2006), recent studies with targeted, endothelial cell-selective deletion of ALK5 reveal normal vascular development and morphology, supporting previous observations that ALK5 is more crucial for smooth muscle rather than endothelial cell function (Park et al., 2008). Moreover, despite the fact that either MMP14 (Lehti et al., 2005) or TGFβ can promote vessel investment by perivascular cells, and that TGFβ alters the accumulation of macromolecules in pancreatic tumors treated with TGFβ inhibitors and has been linked to reduced pericyte coverage (Hirschi et al., 1998; Kano et al., 2007), we did not observe any differences in perivascular cell coverage in Colα1(I)$^{r/r}$ tissues, indicating that TGFβ may activate multiple pathways in perivascular cells leading to stabilization of vasculature.

In vascular smooth muscle cells, TGFβ can bind to ALK5 and activate Smad2 and Smad3 to promote differentiation, and increase contractility and ECM synthesis (Dumont and Arteaga, 2003). Although studies in cultured endothelial cells also described ALK5-mediated increases in Smad3 through an MMP14-dependent activation of TGFβ (Alfranca et al., 2008), we did not observe any changes in vascular leakage in Smad3-deficient mice (N.E.S. and L.M.C., unpublished observations), indicating that ALK5-mediated changes in vascular leakage in vivo probably impact the Smad2 pathway in smooth muscle cells.

Importantly, several studies have found that ALK5 inhibition effectively reduces matrix synthesis and impairs fibrotic reactions in organs including the skin (scleroderma) and kidney (Ishida et al., 2006). Moreover, TGFβ-induced fibroblast or smooth muscle cell contractility can increase the tension on extracellular matrices leading to increased interstitial fluid pressure, which further restricts capillary outflow (Heldin et al., 2004), whereas ALK5 inhibition reduces dermal fibroblast activation in vivo (Ishida et al., 2006). In tumors, drug delivery is influenced considerably by the increased interstitial fluid pressure caused by the increased permeability of tumor vasculature and the absence of functional lymphatics (Minchinton and Tannock, 2006), and is exacerbated further by increased collagen deposition and fibrosis in activated tumor stroma
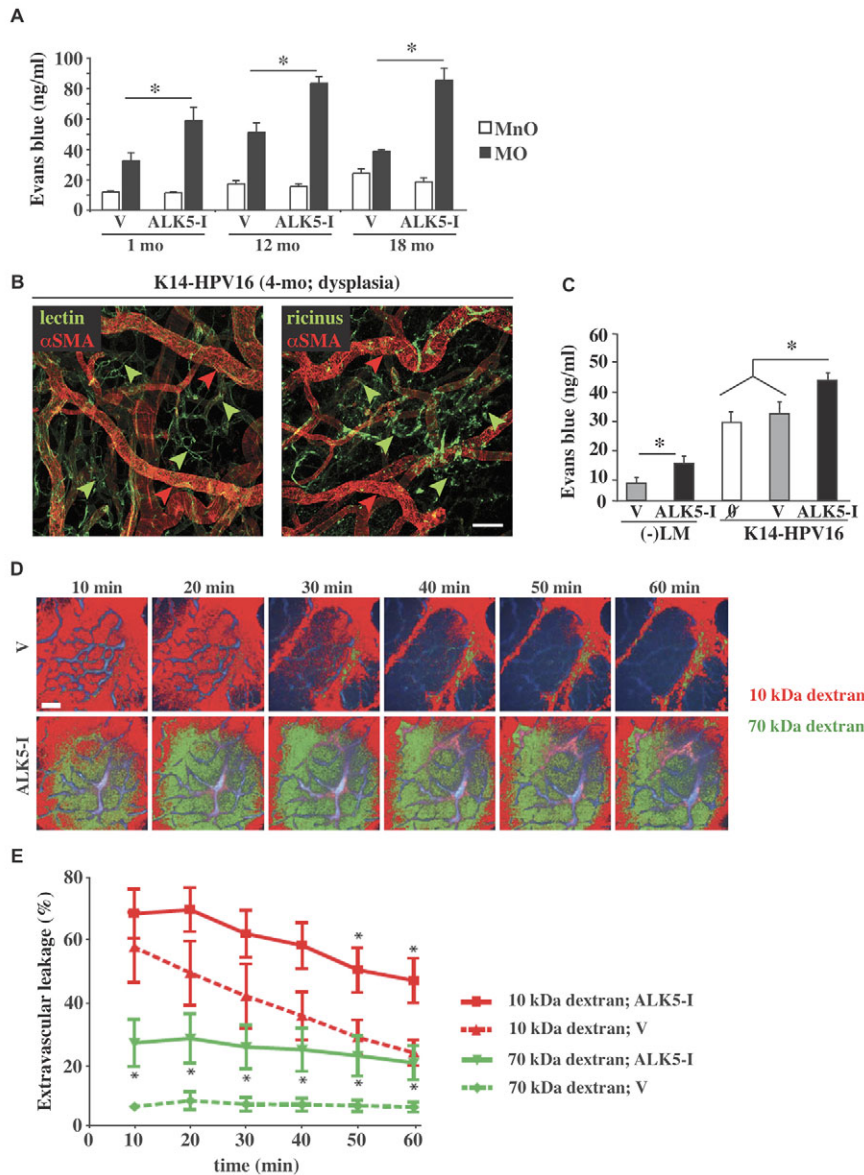
Fig. 6. Inhibition of ALK5 increases vascular leakage in neoplastic tissue. (A) Quantitative assessment of EB leakage in the interstitial ear tissue of 1-, 12- and 18-month-old wild-type C57BL/6 mice treated with mineral oil (MnO; white bars) and mustard oil (MO; black bars), assessed after 5 days of pretreatment with vehicle (DMSO) or an inhibitor to ALK-5 (ALK5-I). Each bar reflects mean ± S.E.M., with five mice per 1- and 12-month-old experimental groups, and four mice for the 18-month-old group. *$P<0.03$. (B) Representative confocal images showing perivascular cell coverage and vascular leakage sites in blood vessels of premalignant angiogenic skin from a K14-HPV16 transgenic mouse (Eichten et al., 2005). On the left, αSMA-positive perivascular cells (red staining, red arrowheads) and blood vessels (green arrowheads) are revealed, showing that the smaller capillary networks lack αSMA-positive perivascular cell coverage. On the right, sites of vascular leakage are revealed by fluorescein-labeled *Ricinus communis* agglutinin I binding (green staining, green arrowheads) in capillaries that are also not covered by αSMA-positive perivascular cells (red staining, red arrowheads). Bar, 100 µm. (C) Quantitative assessment of EB leakage in age-matched 4-month-old, wild-type negative littermate [(–)LM] mice or K14-HPV16 transgenic mice (five mice/experimental group) with premalignant dysplastic skin lesions that were either untreated (Ø), or treated with vehicle (V) versus ALK-5 inhibitor (ALK5-I). *$P<0.01$. (D) Leakage of 70 kDa (green) and 10 kDa (red) dextrans into mammary adenocarcinomas in MMTV-PyMT mice treated with ALK5 inhibitor (ALK-I) or vehicle (DMSO). Dextrans were injected intravenously, together with non-targeted quantum dots (blue) that were used to differentiate between intravascular and extravascular spaces. Images are shown at the indicated times after i.v. injection, with false-coloring of the pixels that are positive for the respective dextrans. Bar, 100 µm. (E) Quantitative assessment of dextran leakage in mammary tumors from 95-day-old MMTV-PyMT mice at the indicated times after i.v. injection of the fluorescent dextrans (five mice/experimental group, error bars reflect S.E.M.). *$P<0.05$.

(Heldin et al., 2004). Reduced type I collagen accumulation enhances drug penetration and drug responses (McKee et al., 2001; Brown et al., 2003; Loeffler et al., 2006; McKee et al., 2006), as does ectopic delivery of interstitial collagenases (Gade et al., 2009). Thus, transient blockade of TGFβ would be expected to not only reduce matrix synthesis, but also to reduce perivascular and stromal cell contractility, leading to reduced interstitial fluid pressure, and improved tissue perfusion and drug delivery.

Indeed, in the MMTV-PyMT transgenic mouse model of mammary carcinogenesis, ALK5 inhibition increased the leakage of high molecular weight dextran into tumor tissue, and increased the retention of low molecular weight dextran in late-stage tumors, indicating that TGFβ and ALK5 regulate vascular paracellular transport mechanisms responsible for the transport of high molecular weight molecules. Although tissue specificity may dictate which intracellular signaling pathway regulates the TGFβ effects on vascular homeostasis, it is clear that multiple tissues, in addition to skin and mammary tissue, respond similarly to TGFβ blockade. In thyroid tumors, inhibition of the TGFβ type II receptor (TGFβRII) leads to reduced interstitial fluid pressure and outward flow of serum proteins from capillaries (Lammerts et al., 2002), and in pancreatic tumors, this leads to the increased accumulation of macromolecules in stroma (Kano et al., 2007).

In Colα1(I)$^{r/r}$ mice, where steady-state levels of bioavailable TGFβ are maintained at elevated levels, we observed a reduction in luminal openings in vessels with a diameter greater than 5 µm. However, in both Colα1(I)$^{r/r}$ mice and aged wild-type mice that accumulate non-enzymatically cross-linked collagen and exhibit vascular dysfunction (Susic, 2007), inhibiting signaling by the ALK5 receptor restores the appropriate vascular response. Thus, the ability of TGFβ to impact matrix synthesis and organization, as well as the contractility of perivascular cells, and to reduce vascular openings, may collectively contribute to restricted vascular leakage in Colα1(I)$^{r/r}$ mice.
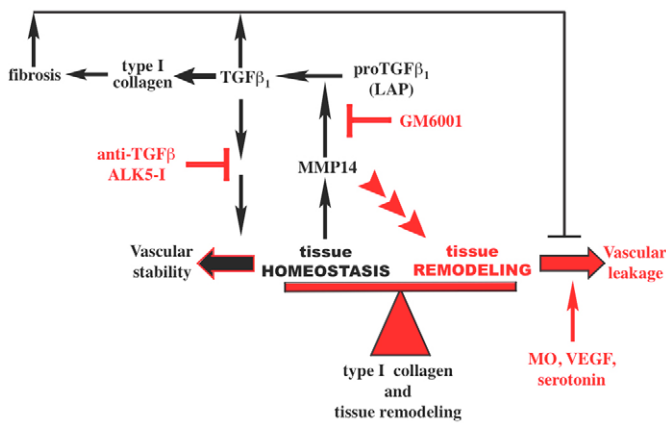
Fig. 7. A model for MMP14- and TGFβ-mediated regulation of vascular homeostasis and leakage during vascular remodeling. The major components of mature capillary networks include endothelial cells, vascular smooth muscle cells and the extracellular matrix. Under homeostatic conditions, these networks are maintained in quiescent states. Following physiologic or pathologic stimulation involving matrix remodeling and/or the increased presence of vascular mediators [VEGF, serotonin, mustard oil (MO)], innate programs are rapidly activated that foster vascular remodeling accompanied by increased leakage of plasma proteins into the tissue interstitium. Increased steady-state levels of MMP14 and/or TGFβ1 lead to the enhanced stability of blood vessels that resist acute leakage following stimulation. By contrast, reducing the steady-state activity of MMP14 or the levels of bioavailable TGFβ, or treatment with ALK5/TGFβ receptor inhibitors, relieves vessel stability rendering homeostatic vessels leaky, and enhances leakage in blood vessels that are already angiogenic and associated with developing tumors.

Stromal regulation of MP activity and TGFβ bioavailability

Our data indicate the existence of a novel feed-forward mechanism by which type I collagen fibrils regulate the activity of MMP14 and the bioavailability of TGFβ. Previous studies have reported that type I collagen upregulates *MMP14* mRNA expression (Haas et al., 1999), and increases cell surface stabilization of the MMP14 protein (Haas et al., 1999), consistent with our data (supplementary material Fig. S1B). Moreover, collagen interactions with the MMP14 hemopexin C domain enhance the formation of multimeric MMP14 complexes, which, in turn, activate proMMP2 (Tam et al., 2002). Typically, MMP14 protein is degraded autolytically following MMP2 activation, and subsequent degradation of collagen further downregulates *MMP14* mRNA expression, whereas addition of metalloproteinase inhibitors leads to prolonged stabilization of MMP14 on the cell surface in cell-based assays (Bernardo and Fridman, 2003). Thus, in Colα1(I)$^{r/r}$ mice, the inability to cleave collagen probably results in surface clustering of MMP14, and stabilized MMP14 enables localized cleavage of the TGFβ LAP to liberate active TGFβ, as well as the enhanced presence of the active form of MMP2.

LAP-TGFβ1 can localize to cell surfaces via integrins (αvβ1, αvβ6 and αvβ5) (Annes et al., 2003) to facilitate TGFβ activation (Cambier et al., 2005). In airway epithelia, LAP-TGFβ also binds to αvβ8, and cleavage of LAP from the TGFβ-αvβ8 complex is mediated by MMP14 (Mu et al., 2002; Araya et al., 2006). As αvβ8 is not expressed by vascular smooth muscle cells (Mu et al., 2002), stabilized collagen fibrils in Colα1(I)$^{r/r}$ mice may directly activate

and stabilize MMP14, which then subsequently activates latent TGFβ. Moreover, although MMP2 can also induce maturation of TGFβ1 or degrade fibrillin, a microfibril-anchoring protein whose loss is linked to activation of TGFβ (Dallas et al., 2002; Mu et al., 2002; Annes et al., 2003), our data demonstrate that MMP14 null mice, but not MMP2 null mice, display vascular phenotypes similar to TGFβ inhibition. Evaluation of steady-state and MO-induced vascular leakage in MMP2-deficient Colα1(I)$^{r/r}$ mice was similar to that found in Colα1(I)$^{r/r}$ mice. Thus, by interfering with the dynamic interplay between collagen, MMP14 and TGFβ, we have identified a novel post-translational pathway that regulates vascular homeostasis.

Summary and perspectives

Findings from this study support several important new concepts (Fig. 7). First, steady-state levels of TGFβ in cutaneous tissue restrict vascular leakage and confer vascular stability. Second, ECM proteins that provide structural integrity also play crucial roles in regulating TGFβ activation, as well as MMP activity (Tam et al., 2002). In a fibrillar state, pericellular type I collagen regulates the expression and activity of the collagenolytic proteases that degrade it (i.e. MMP14 and MMP2) (Overall, 2001), as well as the bioavailability of TGFβ, to directly regulate cell and tissue status. Thus, fibrillar collagen represents an abundant sensor-type molecule endowed with an inherent self-regulating 'switch' that is engaged upon rapid collagen degradation following acute trauma and that, in turn, suppresses a post-translational pathway maintaining vascular stability. Third, these data provide a novel link between type I collagen, MMP14 and TGFβ activation and the regulation of vasodilation and extravasation of plasma proteins – perturbations of which manifest in the pathogenesis of several cutaneous diseases. The present study demonstrates that, in microenvironments where type I collagen fibrils remain stable following acute tissue stimulation, sustained steady-state metalloproteinase activity and TGFβ bioavailability exert dominant control over vascular cells and limit their ability to mount an acute response. Together, these observations support the hypothesis that antagonizing MMP14 or TGFβ activity could repress vascular quiescence in fibrotic tissues, increase plasma protein extravasation in hyperactive tissues, and *normalize* infiltrating responses to resolve fibrotic disorders, whereas enhanced MMP or TGFβ activity may encourage vascular quiescence. Clinically, these data imply that pharmacologic agents that modulate type I collagen fibril status, MMP14 activity and/or TGFβ bioavailability, and/or downstream ALK5 signaling, could profoundly alter tissue hemodynamics that could be therapeutically exploited to improve drug delivery or molecular imaging.

METHODS

Animal husbandry

All mice were maintained within the UCSF Laboratory for Animal Care barrier facility, and all experiments involving animals were approved by the Institutional Animal Care and Use Committee (IACUC) of UCSF. Colα1(I)$^{r/r}$ mice were derived from the colony at Massachusetts General Hospital, Boston, where the mutation was targeted to the J1/129 embryonic stem cells and introduced into the C57BL/6 strain, as described previously (Liu et al., 1995). Backcrosses to FVB/n (N5) mice were performed to create an

inbred line of Colα1(I)$^{r/+}$ mice, and a breeding colony of homozygous mutant Colα1(I)$^{r/r}$ mice was established (UCSF). Controls were the progeny of Colα1(I)$^{+/+}$ breeding pairs that did not possess the mutated gene but were on the same genetic background. The presence of the mutant *Col1a1* allele was assessed by PCR genotyping of tail DNA using oligonucleotide primers that discriminated between the wt allele (5′-TGGACA-ACGTGGTGTGGTC-3′ and 5′-TTGAACTCAGGAATTTAC-CTGC-3′) and the mutant allele (5′-TGGACAACGTG-GTGTGGTC-3′ and 5′-TGGACAACGTGGTGCCGCG-3′) when DNA was successively amplified for 30 cycles at 95°C for 60 seconds, 59°C for 30 seconds, and 72°C for 120 seconds. Mice carrying targeted null mutations in the *Mmp2*, *Mmp8*, *Mmp13* or *Mmp14* genes (Itoh et al., 1997; Zhou et al., 2000; Balbin et al., 2003; Stickens et al., 2004) were individually backcrossed into the FVB/n background for five generations, before they were intercrossed, and homozygous null genotypes were then generated and compared with littermate controls. Gene-switch K14-GLp65/tata.TGFβ1 mice were generated and maintained as described previously (Cao et al., 2002; Lu et al., 2004). Expression of the TGFβ$_1$ transgene (*Tgfb1*) was induced in 4-week-old bigenic mice by topical application of RU486 on ear skin, once a day for 3 days, at a dose of 20 μg/mouse (dissolved in 50 μl of sesame oil); mice were then analyzed on day 4. K14-HPV16 and MMTV-PyMT mice were maintained in the FVB/n strain and analyzed as described previously (Guy et al., 1992; Coussens et al., 1996).

Neutralization of TGFβ activity in vivo was accomplished by intraperitoneal (i.p.) injections of pan-specific TGFβ antibody (R&D Systems, MN; #AB-100; 1.0 mg/ml in sterile PBS, pH 7.4), at 5.0 mg/kg body weight, at 120, 96 and 24 hours before MO challenge. Control animals received normal rabbit IgG (R&D Systems; #AB-105-C). Five animals per cohort were injected and the experiment was repeated three times. GM6001 {N-[(2R)-2-hydroxyamidocarbonylmethyl-0-4-methylpentanoyl]-L-tryptophan ethylamide} (Galardy et al., 1994), a broad, class-specific MP inhibitor (Chemicon International, CA), was administered i.p., at 100 mg/kg body weight, as a 20 mg/ml slurry in 4.0% carboxymethylcellulose (CMC) in 0.9% PBS, daily, for 3 days prior to cutaneous challenge. Controls were treated with a daily injection of 4% CMC in PBS. Four animals per cohort were injected and the experiment was repeated four times. This concentration of GM6001 has been demonstrated to inhibit in vivo MP activity (Zheng et al., 2000). Pharmacological inhibition of ALK5 was achieved using the ALK5 kinase inhibitor [3-(pyridin-2-yl)-4-(4-quinonyl)]-1H-pyrazole (Calbiochem, San Diego, CA), which was administered i.p., at 1.0 mg/kg, in 2% DMSO in sterile PBS every other day for 6 days. Control mice received equivalent i.p. injections of the solvent vehicle DMSO. For biodistribution studies with dextran, mice were intravenously given 100 μl of lysine-fixable dextran 10,000 kDa Alexa Fluor 647 at 2.0 mg/ml (Molecular Probes) and 50 μl dextran 70,000 kDa tetramethylrhodamine at 4.0 mg/ml (Molecular Probes), and were studied 3 hours later. All analyses used age-matched mice and five mice per treatment group, and all experiments were repeated a minimum of three separate times. For all other experiments, analyses were conducted in triplicate on cohorts containing at least three mice and *P* values of <0.05 were considered significant. All animal experiments were conducted in accordance with procedures approved by the IACUC, UCSF.

Miles assay
Evans Blue (EB) dye (30 mg/kg in 100 μl PBS; Sigma-Aldrich, St Louis, MO) was injected into the tail vein of 7- to 8-week-old mice in all analyses, except for MMP14 null animals where, owing to early neonatal lethality, 17-day-old mice were injected i.v. with EB dye retro-orbitally, and assayed as described below. In some experiments, after 1 minute, 30 μl of 5% MO (phenyl isothiocyanate, 98%, Sigma-Aldrich) diluted in MnO (Sigma-Aldrich) was applied to the dorsal and ventral surfaces of the ear; the application process was repeated 15 minutes later. Isoflurane-anesthetized mice were photographed 30 minutes after the injection of EB dye. Anesthetized mice were then cardiac-perfused (see below), their ears removed, and blotted dry and weighed. EB dye was extracted from ears in 1 ml of formamide, for 12-48 hours at 60°C, and measured spectrophotometrically at 610 nm in a SpectraMax 340 (Molecular Devices, Sunnyvale, CA). Data are expressed as mean ± S.E.M. Comparisons of the amounts of dye extravasation were evaluated by Mann-Whitney statistical test with *P* values less than 0.05 considered significant. In some experiments, 5 minutes prior to the infusion of EB dye, shaved 5- to 7-week-old mice were injected intradermally (10 μl) with one of the following agents at the concentrations shown: VEGF$_{120}$ (R&D Systems), VEGF$_{164}$ (Chemicon International), histamine (Calbiochem) or serotonin (Sigma-Aldrich). The appearance of a blue spot was monitored for 30 minutes, at which time mice were euthanized, cardiac-perfused, photographed, and the area of skin surrounding the site of injection was excised (~5 mm^2), photographed, and the EB dye extracted as above.

Vascular perfusions and fluorescent angiography
Isoflurane-anesthetized mice were injected with fluorescein-labeled *Lycopersicon esculentum* lectin (100 μl, 2 mg/ml; Vector Laboratories, Burlingame, CA) or rhodamine-labeled *Ricinus communis* agglutinin I (50 μl, 5.0 mg/ml; Vector Laboratories) into the femoral vein, as described (Thurston et al., 1996; Thurston et al., 1998). Two minutes after lectin injection, mice were perfused with fixative (1% paraformaldehyde plus 0.5% glutaraldehyde in PBS, pH 7.4, at 37°C) through the ascending aorta for 2 minutes to fix the vasculature and flush out non-adherent leucocytes. Confocal images were acquired on a Zeiss LSM 510 META NLO with an ultrafast, tunable Coherent Ti:Sa MIRA laser with Verdi pump for multi-photon excitation.

Immunohistochemistry
Immunodetection of α-smooth muscle actin was performed on tissue pieces following injection of *Ricinus communis* lectin and cardiac perfusion, as described above. Tissue pieces were fixed in 4% paraformaldehyde for 4 hours in the dark at 4°C, with gentle agitation, followed by several washes in 4°C PBS, before being permeabilized in 0.3% Triton X-100 overnight with gentle agitation at 4°C. Tissue pieces were then incubated with a Cy3-labeled anti-α-smooth muscle actin monoclonal antibody (mAb) (Sigma-Aldrich; Clone 1A4 #C6198, 1:500) diluted in 5% normal goat serum, 2.5% BSA, 0.3% Triton X-100 in PBS, overnight at 4°C on a rotating platform, followed by extensive washing in 4°C PBS and mounting with Vectashield (Vector Laboratories) mounting medium. Images were acquired on a Zeiss LSM 510 META NLO with an ultrafast, tunable Coherent Ti:Sa MIRA laser with Verdi

pump for multi-photon excitation. Immunodetection of TGFβ in ear skin was performed on formalin-fixed, 5-μm, paraffin-embedded sections incubated with a mouse monoclonal anti-TGFβ antibody (R&D Systems; clone: 1D11) at a 1:50 dilution, revealed with biotinylated goat anti-mouse secondary antibody, at a 1:200 dilution, and counterstained in 1.0% methyl green and mounted with Cytoseal 60.

Immunofluorescence (IF) for αSMA and ALK5 was performed on 10-μm cryo-frozen tissue sections of ear skin that were fixed for 10 minutes with cold acetone, blocked for 30 minutes, and incubated with primary antibodies (ALK5, 1:50 dilution; Abcam #31013; αSMA clone 1A4, 1:100 dilution; Sigma) overnight at 4°C, followed by successive PBS washes and the application of secondary antibodies (1:500). Following further PBS washes, the sections were mounted with Vectashield media containing DAPI (Vector) and analyzed using a confocal microscope LSM 510 with a 63× oil objective, and images were then analyzed with a Zeiss LSM image examiner.

Immunodetection of MMP14 protein in collagen matrices was performed after incubation of cells in three-dimensional (3D) collagen gels for 18 hours without serum. The medium was then aspirated from each well and the cells were immediately fixed with 2.0% paraformaldehyde (2% PFA in PBS, pH 7.4, freshly prepared) for 20 minutes at room temperature (RT), then permeabilized with PBS containing 0.5% Triton X-100 for 10 minutes at 4 C, washed three times with PBS-glycine (130 mM NaCl, 7.0 mM Na_2HPO_4, 3.5 mM NaH_2PO_4, 10 mM glycine), and then blocked with 200 μl/well of IF buffer (130 mM NaCl, 7.0 mM Na_2HPO_4, 3.5 mM NaH_2PO_4, 0.1% BSA, 0.2% Triton X-100, 0.05% Tween-20) with 10% goat serum for 1 hour at RT. The primary rabbit polyclonal anti-MT1-MMP (hinge region) antibody (AB815, Chemicon), which was diluted at 1:250 in IF Buffer with 10% goat serum, was incubated overnight at 4°C. Samples were washed three times with IF buffer for 20 minutes each, followed by incubation with Alexa Fluor 488 goat anti-rabbit antibody, diluted 1:200 in IF buffer with 10% goat serum, for 45 minutes. Cells were then washed three times with IF buffer, cover slipped with the gel, and mounted in Vectashield with DAPI mounting medium, and allowed to air dry. Once dry, slides were observed by laser confocal microscopy using a Zeiss LSM META.

Protein analysis
VEGFR2
Tissue pieces (5 mm^2) were collected from ears, or shaved back skin, following the injection (i.d.) of 10 μl of 10 ng $VEGF_{164}$ or 0.1% BSA in PBS. Tissues were pulverized in liquid nitrogen (N_2), followed by lysis in ice-cold buffer containing 20 mM Tris, pH 7.6, 150 mM NaCl, 1.0 mM EDTA, 50 mM NaF, 1.0% Triton X-100, 0.5% Na-deoxycholate, 0.1% SDS, 2.0 mM Na_2VO_4, 10 μg/ml aprotinin and 1.0 mM phenylmethylsulfonylfluoride, and centrifuged at 10,000 rpm (9503 × *g*) for 30 minutes at 4°C. The supernatants were re-centrifuged at 10,000 rpm for 30 minutes at 4°C. Lysates were then incubated in a slurry of heparin-sepharose CL-6B (Pharmacia, Peapack, NJ) and incubated overnight, rocking at 4°C, and then centrifuged and equilibrated to 150 mM NaCl. Protein was dialyzed against PBS and quantified using the Bio-Rad protein assay system (Bio-Rad, Hercules, CA). Before immunoprecipitation, BSA was added to the pre-cleared lysates at 0.5%. Equal amounts of protein (1.0 mg) from lysates were used for immunoprecipitations and western blotting. Incubation of tissue lysate with goat anti-Flk-1

(Santa Cruz Biotechnology, Santa Cruz, CA) followed by protein-G sepharose beads was performed for 2 hours at 4°C. Immunoprecipitates were washed three times with 20 mM Tris (pH 7.6), 150 mM NaCl and 0.1% Triton X-100, and bound proteins were eluted by boiling in 1× SDS-PAGE sample buffer for 5 minutes, followed by electrophoresis on 10% SDS-PAGE under reducing conditions. The resolved proteins were transferred to a nitrocellulose membrane (BA-S85; Schleicher & Schuell BioScience, Inc., Keene, NH). Anti-phosphotyrosine PY-20 (Upstate Biotechnology, Lake Placid, NY) and anti-Flk-1 (Santa Cruz Biotechnology) antibodies were used on western blots. Immunodetection was performed by incubation with specific peroxidase-conjugated secondary antibodies followed by enhanced chemiluminescence (ECL) (Amersham Biosciences, Piscataway, NJ).

TGFβ ELISA
Tissues were pulverized in liquid N_2 and solubilized in lysis buffer containing 50 mM Tris, 75 mM NaCl, 10 mM EDTA, protease inhibitor cocktail mix without EDTA (Roche, Indianapolis, IN), 0.01 mg/ml aprotinin (Sigma-Aldrich), 0.1 mg/ml leupeptin (Sigma-Aldrich) and 10 mM phenylmethylsulfonyl fluoride (PMSF) (Sigma-Aldrich) using a 2.0 ml tissue grinder (Fisher Scientific, Pittsburgh, PA), followed by centrifugation at 10,000 × *g* for 30 minutes at 4°C. Protein concentration was determined using the Bio-Rad DC Protein assay reagent according to the manufacturer's instructions (Bio-Rad). To determine total levels of $TGFβ_1$ in tissue lysates, a standard protocol for quantitative sandwich enzyme immunoassay was used. For ELISA analysis, a monoclonal antibody specific for active $TGFβ_1$, $β_2$ and $β_3$ (1.0 μg/ml in PBS; R&D Systems; MAB1835) was used to pre-coat maxisorb immunoplates (Nalge Nunc International, Rochester, NY) overnight at RT. Lysates (100 μg) were activated by adding 1.0 N HCl (1:25) and incubated for 1 hour at 4°C with gentle agitation. Acidified samples were neutralized by adding 1.0 N NaOH (1:25) and diluted with ELISA sample buffer (1× PBS, 0.05% Tween-20, 1.4% fatty acid-free BSA). Samples were then added to pre-coated maxisorb immunoplates and incubated for 3 hours at RT, which was followed by the addition of biotinylated anti-$TGFβ_1$ antibody (200 ng/ml; R&D Systems; BAF240) and incubation overnight at 4°C. Avidin-peroxidase conjugate (1:1000; Sigma-Aldrich) was added for 1 hour at RT followed by a 20-minute incubation with o-phenylenediamine (OPD) substrate at RT in the dark (Sigma-Aldrich). The reaction was stopped by addition of 1.0 M H_2SO_4 and absorbance was measured at 450 nm (570 nm for background corrections) on a Molecular Device Spectra Max 340. Recombinant human $TGFβ_1$ (R&D Systems) was used as a standard control. Six tissues samples per genotype were analyzed and all samples were analyzed in duplicate.

TGFβ and LAP
For immunoprecipitation of TGFβ, 4.2 mg of protein lysates were pre-cleared with protein A-agarose beads (Roche) for 1 hour at 4°C, followed by centrifugation at 3000 rpm (5 minutes). The supernatant was then incubated with 2.0 μg of antibody for $TGFβ_1$, $β_2$ and $β_3$ (R&D Systems; MAB1835) or MMP14 (Chemicon International; AB8102, catalytic domain; MAB3317, hemopexin domain) for 3 hours at 4°C in HNTG buffer (20 mM HEPES, pH 7.5, 150 mM NaCl, 0.1% Triton X-100, 10% glycerin, 10 mM Na pyrophosphate, 10 mM NaF, 1 mM Na-o-vanadate, 1 mM PMSF

and 10 μg/ml aprotinin). After incubation with protein agarose G or A beads (Roche) for an additional hour at 4°C, the lysates bound to agarose beads were washed three times with HNTG buffer, and bound proteins were eluted by boiling in 1× reduced SDS-PAGE sample buffer for 5 minutes and then centrifuged at 13,000 rpm for 10 minutes. Tissue lysates (20 μg for LAP) or eluted immunoprecipitated complexes were separated by electrophoresis on 10% SDS polyacrylamide gels, and transferred to nitrocellulose membranes overnight at 4°C. Membranes were blocked, incubated with primary antibodies for 1-2 hours at RT, washed, and then incubated with secondary antibodies (Bio-Rad; goat anti-rabbit- or goat anti-mouse-HRP conjugate 1:2000) or strepavidin-HRP conjugate (Sigma-Aldrich; 1:20,000) for 1 hour at RT. Membranes were then washed and developed by using an ECL kit (Amersham Biosciences). Biotinylated LAP antibodies (R&D Systems; BAF246, 1:1000), biotinylated anti-TGFβ₁ antibodies (R&D Systems; BAF240, 1:1000) and antibodies to MMP14 (Oncogene Science, Cambridge, MA, 1M397, 1:1000; Chemicon International, AB8104, 1:1000) were used for detection on membranes. For the loading control in LAP western analysis, a rat monoclonal antibody (AbCam, Cambridge, MA; YL1/2, 1:5000) against α-tubulin and a goat anti-rat-HRP (Pierce, Rockford, IL; 1:2000) were used.

TGFβ bioassay

TGFβ bioavailabilty in tissue lysates from mice, and in conditioned medium from MDA-MB-MMP14 cells grown in either +/+ or r/r collagen matrices, was assayed using mink lung epithelial cells (MLEC) transfected with a luciferase reporter gene under the control of the TGFβ-sensitive promoter (PAI-1), and maintained as described previously (Abe et al., 1994). PAI-1-MLEC cells (2.5×10^4) were cultured in 96-well culture plates in 500 μl DMEM containing 10% FBS, and allowed to attach for 6 hours at 37°C. After two PBS washes, the medium was replaced with tissue lysate or conditioned medium. Tissue lysates were prepared as described above for ELISA. 50 μg of total proteins was diluted in incubation medium [high-glucose DMEM, 0.2% BSA (Fraction V, fatty acid-free; Calbiochem), penicillin/streptomycin, 2.0 mM L-glutamine, 250 μg/ml G-418 sulfate] and incubated with PAI-1-MLEC cells for 20 hours in the presence or absence of anti-TGFβ antibody (15 μg/ml; R&D Systems; clone 1D11). For conditioned medium analyses, MDA-MB-231 cells were grown in either +/+ or r/r collagen, as described above, and incubated in the presence or absence of GM6001 (10 μM; Chemicon International) or anti-TGFβ antibody (15 μg/ml). Conditioned medium (50 μl) was diluted in 50 μl of incubation medium and incubated with PAI-1-MLEC cells for 20 hours. Cells were washed twice with PBS, incubated with lysis buffer (Promega, Madison, WI), and luciferase activity was then measured using a Luciferase Assay System kit (Promega) following the manufacturer's instructions. Relative luminescence units (RLU) were calculated as an average from triplicate wells per culture condition and repeated in triplicate.

RNA analysis

Total RNA was extracted from shaved back skin or ear pieces with TRIzol reagent (Invitrogen, New York, NY), according to the manufacturer's recommendations, by powdering fresh-frozen tissue samples in liquid N₂, homogenizing with a microtube pestle (USA Scientific, Ocala, FL), shearing by multiple passages through a syringe and 21-gauge needle (Becton Dickinson, Franklin Lakes, NJ),

followed by chloroform extraction, isopropanol precipitation, and an ethanol wash. Northern blot analysis was performed using standard methods with 10 μg of total cellular RNA. Probes were generated by random primed labeling of DNA isolated from plasmids using standard methodology (Maniatis et al., 1982). Northern blots were hybridized at 65°C overnight in Church buffer (0.5 M sodium phosphate, pH 7.2, 1.0 mM EDTA, 7.0% w/vol SDS, 250 μg/ml tRNA), and subsequently washed at 62°C in 2× SSC containing 1.0% SDS. The probes used for hybridization were: a 335 bp fragment of *Mmp2* (EMBL: M84324; position: 2053-2387 bp), a 335 bp fragment of *Mmp14* (EMBL: NM_008608; position: 54-388 bp), a 669 bp fragment of *Timp2* (EMBL: X62622; position: 2-670 bp), a 974 bp fragment of *Tgfb1* (EMBL: M13177; position: 421-1395 bp) and a 207 bp fragment for 18S RNA as a loading control (EMBL: J00623; position: 13-219 bp). Hybridized filters were exposed overnight on phosphor screens, analyzed in a Phosphoimager (Molecular Dynamics, Sunnyvale, CA; Storm 860, ImageQuant 5.2 software), and then additionally exposed for 1-3 days on Kodak Biomax MS films (Kodak, Rochester, NY) with an intensifier screen at −80°C.

Substrate conversion assay

Shaved dorsal skin pieces isolated from 5–8-week-old mice were pulverized in liquid N₂ and solubilized in 500 μl buffer [0.25 M sucrose, 5 mM Tris, pH 7.5, protease inhibitor cocktail mix without EDTA (Roche), 0.25 mg/ml Pefablock (Roche), 0.01 mg/ml aprotinin (Sigma-Aldrich)] and centrifuged at $800 \times g$ for 15 minutes at 4°C. Supernatants were then centrifuged for 1 hour at $100,000 \times g$ at 4°C, and pellets were resuspended in 100 μl solubilization buffer and homogenized by sonication at 4°C. Protein concentration was determined using the Bio-Rad DC Protein assay reagent according to the manufacturer's instructions (Bio-Rad). Lysate buffers were then exchanged with 10 mM Tris, pH 7.5, using Micro Bio-Spin chromatography columns (Bio-gelP-6; Bio-Rad). To determine gelatinolytic activity in tissue lysates, supernatant fractions (50 μg) were incubated with 400 ng DQ-gelatin (Molecular Probes) in reaction buffer (50 mM Tris, pH 7.6, 150 mM NaCl, 5.0 mM CaCl₂, 0.2 mM sodium azide and 0.05% BrJ35) at 37°C. Reactions were analyzed for 5 hours at 37°C and fluorescence measured (excitation 485 nm, emission 530 nm) every 3 minutes using a microplate spectrofluorometer (SpectraMax Gemini EM, Molecular Devices) operated by SoftMax Pro 4.1 software. Values shown represent the mean ± S.E.M. from three tissue pieces and are representative of analyses performed in triplicate. Each experiment was repeated three independent times.

Substrate zymography

Tissue samples (ear) from 5–8-week-old mice were weighed and homogenized (1:8 weight to volume) in lysis buffer containing 50 mM Tris-HCl (pH 8.0), 150 mM NaCl, 0.1% NP-40, 0.5% deoxycholate and 0.1% SDS. Soluble and insoluble extracts were separated by centrifugation ($10,000 \times g$) and subsequently stored at −80°C. Equivalent amounts of soluble extract were analyzed by gelatin zymography (Herron et al., 1986a) on 10% SDS-polyacrylamide gels co-polymerized with substrate (1.0 mg/ml of gelatin) in sample buffer (2% SDS, 50 mM Tris-HCl, 10% glycerol, 0.1% Bromophenol Blue, pH 6.8). After electrophoresis, gels were washed three times for 30 minutes in 2.5% Triton X-100, then washed three times for 15 minutes in ddH₂O, incubated overnight

at 37°C in 50 mM Tris-HCl and 10 mM CaCl$_2$ (pH 8.2), and then stained in 0.5% Coomassie Blue and destained in 20% methanol, 10% acetic acid. Negative staining indicates the location of active protease bands. Exposure of pro-enzymes within tissue extracts to SDS during the gel separation procedure leads to activation without proteolytic cleavage (Herron et al., 1986b).

Cell-based MMP assay

To prepare collagen gels for culture experimentation, mouse tail collagen was purified as described previously (Miller and Rhodes, 1982) and quantified by determination of hydroxyproline content (Woessner, 1961; Bergman and Loxley, 1963). Subsequently, eight volumes of +/+ and r/r collagen (4.4 mg/ml) were neutralized by the addition of one volume of 10× PBS containing 0.005% Phenol Red and one volume of NaOH. 50 µl of MDA-MB-231 breast carcinoma cells expressing a full-length human *MMP14* cDNA (Tam et al., 2004), at 5×10^6 cells/ml in serum-free DMEM, were added to 200 µl of neutralized +/+ and r/r collagen. The collagen/cell suspensions were mixed thoroughly and then four 50 µl aliquots were added per well into a 96-well culture dish (Corning, Corning, NY) and incubated at 37°C for 1 hour to allow collagen polymerization. 100 µl of DMEM containing 10% fetal bovine serum was then added to cells and incubated at 37°C for 18 hours. Collagen gels were washed with 200 µl serum-free DMEM, and cells were then incubated in 100 µl serum-free DMEM containing human proMMP2, since the MDA-MB-231 cells essentially express no MMP2. Conditioned medium was harvested after 48 hours and collagen gels were washed in 200 µl of PBS. 50 µl of non-reducing SDS-PAGE sample buffer was then added to collagen gels to extract the collagen-bound MMP2 and then, after collection, the sample buffer was used to bring the total volume to 200 µl. Equivalent amounts of supernatants and collagen-bound MMP2 extracts were analyzed by gelatin zymography and incubated for 4 hours at 37°C.

In vivo measurements of vascular leakage

MMTV-PyMT mice (Guy et al., 1992) (approximately 100 days old) were treated with the ALK5 inhibitor [3-(Pyridin-2-yl)-4-(4-quinonyl)]-1H-pyrazole (Calbiochem), which was given i.p. every other day at 1.0 mg/kg in 2% DMSO in sterile PBS. Control mice received vehicle alone. On day 6 of treatment, tumors were imaged in live mice as described previously (Egeblad et al., 2008). Briefly, the mice were anesthetized and the inguinal mammary gland containing a tumor was surgically exposed. Images from live mice were acquired using a Fluor 10×/0.5 NA lens and a micro-lensed spinning disk confocal microscope (Solamere Technology Group, Salt Lake City, UT) equipped with argon and krypton lasers (Dynamic Lasers, Salt Lake City, UT). Images were collected with an ICCD camera (XR-Mega-10EX S-30, Stanford Photonics, Palo Alto, CA). The anesthetized mice were injected i.v., into the tail vein, with 100 µl sterile PBS containing 1.0 mg/ml 10 kDa Alexa Fluor 647-conjugated dextran, 2.0 mg/ml 70 kDa rhodamine-conjugated dextran and 0.4 µM Qtracker 705 non-targeted quantum dots (all from Invitrogen). Five animals in each group were imaged and the tumors were between 6-11 mm in diameter.

From the acquired image sets, maximum intensity projections of 16-µm optical sections were generated using Bitplane Imaris (version 5.7 for Windows X64). To determine dextran leakage, these sets were analyzed further using Improvision Volocity (version 4.1.0

for Windows). Pixel intensities in the quantum dot channel that were below 125% of the mean background intensity were used to define the extravascular space (negative for quantum dots). Leakage of 10 kDa or 70 kDa dextran to the extravascular space was defined as the percentage of the extravascular space with pixel intensities above 150% of the mean background intensity levels. From each mouse, 3-5 fields of view (imaged in parallel) were analyzed. The average percentage of extravascular leakage for the five mice in each group is reported. Differences in dextran leakage between controls and ALK5 inhibitor-treated mice were compared using Student's *t*-test (two-tailed, unequal variance) using GraphPad Prism 4 software.

Statistical analysis

Statistical analyses were performed using GraphPad Prism and/or InStat software. The specific tests used were Student's *t*-test, Mann-Whitney (unpaired, nonparametric, two-tailed) test, and unpaired *t*-test with Welch's correction. *P* values <0.05 were considered statistically significant.

TRANSLATIONAL IMPACT

Clinical issue
In patients with locally advanced solid tumors, the first-line treatment is often neo-adjuvant or pre-operative chemotherapy, which helps shrink tumors before surgery, allowing for more conservative surgical approaches and reducing the potential for developing systemic disease. However, despite aggressive chemotherapy, long-term survival for many patients remains poor, in part owing to limitations with the targeting and accumulation of cytotoxic drugs in tumor tissue.

The vasculature of solid tumors is abnormal, both in terms of vessel architecture and the dynamics of blood flow. Permeable heterogeneous vessel walls allow the leakage of proteins and fluid that, coupled with the inefficiency of lymphatic drainage, could be exploited to develop novel, enhanced drug delivery strategies that are therapeutically selective and improve clinical outcome.

Results
This work describes a previously unappreciated role for transforming growth factor beta (TGFβ) in regulating vascular stability and vessel permeability in solid tumors. Using mouse models, the authors demonstrate an endogenous pathway that regulates normal vascular permeability, which is controlled by perivascular collagen, the metalloproteinase enzyme MMP14, and TGFβ. In wild-type mice, inhibitors of either MMP14 or TGFβ signaling induce blood vessel permeability. Conversely, enhanced MMP14 or TGFβ activity in the mouse epidermis decreases leakage across cutaneous vessels. This pathway remains functional during tumor progression, as acute blockade of either MMP14 or TGFβ signaling transiently alters vessel stability, 'opening' vascular beds and promoting intravenous delivery of high molecular weight compounds to the tumor.

Implications and future directions
The delivery of standard therapeutic agents or diagnostic molecular imaging agents to tumor tissue may be enhanced by transient blockade of the TGFβ pathway. If so, this could advance disease therapy and/or diagnostic imaging, not only in cancer medicine, but also in fibrotic disorders such as scleroderma and kidney failure.

doi:10.1242/dmm.005314

COMPETING INTERESTS

The authors declare no competing financial interests.

AUTHOR CONTRIBUTIONS

N.E.S. performed experiments to evaluate MMP-deficient and bigenic TGFβ mice for altered dynamics of vascular stability and vascular leakage; performed functional experiments to define the role of ALK5 and SMAD3 in mediating vascular stability; and evaluated MMP14 in cell-based assays for activation of latent TGFβ and regulation by collagen fibrils. K.D. performed experiments to evaluate the functional role for TGFβ in mediating vascular stability using in vivo and ex vivo assays. L.v.K. performed the initial vascular leakage experiments in mutant collagen mice exposed to various stimulants. M.E. designed experiment to assess the kinetics of vascular leakage in mammary carcinomas with L.M.C., conducted the experiment in real time, and established parameters for data analysis. N.I.A. and I.C. worked together to evaluate age-associated changes in vascular homeostasis and the response to acute stimulation in the presence of ALK5 blockade. J.W. assisted M.E. with real-time imaging and quantitative data analysis of vascular leakage in mammary carcinomas. S.J. assisted M.E. with real-time imaging of vascular leakage in mammary carcinomas. L.K. maintained the animal colony, backcrossed mice onto the FVB/n strain, generated all genetic intercrosses, and performed all genotype analyses for all mice throughout the project. J.L. assisted L.v.K. with fluorescent angiography and animal husbandry studies. J.S. performed whole-mount immunohistochemistry to visualize blood vessels and perivascular cells in homeostatic, MO-stimulated and neoplastic tissues. C.J.M. performed the ex vivo cell-based assay with MDA-MB-231 cells expressing MMP14 to validate collagen stabilization of MMP14 and processing of latent MMP2. C.M.O.'s laboratory generated the MDA-MB-231 cells expressing MMP14 and, together with L.M.C., designed the cell-based assay in mutant collagen to assay MMP2 activation. S.M.K. provided mutant collagen mice and consulted on the phenotype of mice throughout the project. Z.W. consulted with L.M.C. over the entire length of the project, following acquisition of the altered phenotype in mutant collagen mice, and designed the spinning disk microscopic approach for real-time imaging with M.E. N.B. worked with L.M.C. to design experiments with aged mice and mammary tumor-bearing mice, and co-wrote the manuscript with L.M.C. L.M.C. conceived the project and had direct oversight of all experimental designs, and wrote the manuscript with consultation from N.B.

SUPPLEMENTARY MATERIAL

Supplementary material for this article is available at http://dmm.biologists.org/lookup/suppl/doi:10.1242/dmm.003863/-/DC1

REFERENCES

Abe, M., Harpel, J. G., Metz, C. N., Nunes, I., Loskutoff, D. J. and Rifkin, D. B. (1994). An assay for transforming growth factor-beta using cells transfected with a plasminogen activator inhibitor-1 promoter-luciferase construct. *Anal. Biochem.* **216**, 276-284.

Alfranca, A., Lopez-Oliva, J. M., Genis, L., Lopez-Maderuelo, D., Mirones, I., Salvado, D., Quesada, A. J., Arroyo, A. G. and Redondo, J. M. (2008). PGE2 induces angiogenesis via MT1-MMP-mediated activation of the TGFbeta/Alk5 signaling pathway. *Blood* **112**, 1120-1128.

Annes, J. P., Munger, J. S. and Rifkin, D. B. (2003). Making sense of latent TGFbeta activation. *J. Cell Sci.* **116**, 217-224.

Araya, J., Cambier, S., Morris, A., Finkbeiner, W. and Nishimura, S. L. (2006). Integrin-mediated transforming growth factor-{beta} activation regulates homeostasis of the pulmonary epithelial-mesenchymal trophic unit. *Am. J. Pathol.* **169**, 405-415.

Balbin, M., Fueyo, A., Tester, A. M., Pendas, A. M., Pitiot, A. S., Astudillo, A., Overall, C. M., Shapiro, S. D. and Lopez-Otin, C. (2003). Loss of collagenase-2 confers increased skin tumor susceptibility to male mice. *Nat. Genet.* **35**, 252-257.

Bergers, G., Brekken, R., McMahon, G., Vu, T. H., Itoh, T., Tamaki, K., Tanzawa, K., Thorpe, P., Itohara, S., Werb, Z. et al. (2000). Matrix metalloproteinase-9 triggers the angiogenic switch during carcinogenesis. *Nat. Cell Biol.* **2**, 737-744.

Bergman, I. and Loxley, R. (1963). Two improved and simplified methods for the spectrophotometric determination of hydroxyproline. *Anal. Chem.* **35**, 1961-1965.

Bernardo, M. M. and Fridman, R. (2003). TIMP-2 (tissue inhibitor of metalloproteinase-2) regulates MMP-2 (matrix metalloproteinase-2) activity in the extracellular environment after pro-MMP-2 activation by MT1 (membrane type 1)-MMP. *Biochem. J.* **374**, 739-745.

Bhushan, M., Young, H. S., Brenchley, P. E. and Griffiths, C. E. (2002). Recent advances in cutaneous angiogenesis. *Br. J. Dermatol.* **147**, 418-425.

Brown, E., McKee, T., diTomaso, E., Pluen, A., Seed, B., Boucher, Y. and Jain, R. K. (2003). Dynamic imaging of collagen and its modulation in tumors in vivo using second-harmonic generation. *Nat. Med.* **9**, 796-800.

Cambier, S., Gline, S., Mu, D., Collins, R., Araya, J., Dolganov, G., Einheber, S., Boudreau, N. and Nishimura, S. L. (2005). Integrin alpha(v)beta8-mediated activation of transforming growth factor-beta by perivascular astrocytes: an angiogenic control switch. *Am. J. Pathol.* **166**, 1883-1894.

Cao, T., He, W., Roop, D. R. and Wang, X. J. (2002). K14-GLp65 transactivator induces transgene expression in embryonic epidermis. *Genesis* **32**, 189-190.

Coussens, L. M., Hanahan, D. and Arbeit, J. M. (1996). Genetic predisposition and parameters of malignant progression in K14- HPV16 transgenic mice. *Am. J. Pathol.* **149**, 1899-1917.

Dallas, S. L., Rosser, J. L., Mundy, G. R. and Bonewald, L. F. (2002). Proteolysis of latent transforming growth factor-beta (TGF-beta)-binding protein-1 by osteoclasts. A cellular mechanism for release of TGF-beta from bone matrix. *J. Biol. Chem.* **277**, 21352-21360.

Dickson, M. C., Martin, J. S., Cousins, F. M., Kulkarni, A. B., Karlsson, S. and Akhurst, R. J. (1995). Defective haematopoiesis and vasculogenesis in transforming growth factor-beta 1 knock out mice. *Development* **121**, 1845-1854.

Drab, M., Verkade, P., Elger, M., Kasper, M., Lohn, M., Lauterbach, B., Menne, J., Lindschau, C., Mende, F., Luft, F. C. et al. (2001). Loss of caveolae, vascular dysfunction, and pulmonary defects in caveolin-1 gene-disrupted mice. *Science* **293**, 2449-2452.

Dumont, N. and Arteaga, C. L. (2003). Targeting the TGF beta signaling network in human neoplasia. *Cancer Cell* **3**, 531-536.

Egeblad, M., Shen, H. C., Behonick, D. J., Wilmes, L., Eichten, A., Korets, L. V., Kheradmand, F., Werb, Z. and Coussens, L. M. (2007). Type I collagen is a genetic modifier of matrix metalloproteinase 2 in murine skeletal development. *Dev. Dyn.* **236**, 1683-1693.

Egeblad, M., Ewald, A. J., Askautrud, H. A., Truitt, M. L., Welm, B. E., Bainbridge, E., Peeters, G., Krummel, M. F. and Werb, Z. (2008). Visualizing stromal cell dynamics in different tumor microenvironments by spinning disk confocal microscopy. *Dis. Model. Mech.* **1**, 155-167.

Eichten, A. E., Shen, H.-C. J. and Coussens, L. M. (2005). Three-dimensional visualization of blood and lymphatic vasculature in tissue whole mounts using confocal microscopy. In *Current Protocols in Cytometry* (ed. J. P. Robinson), pp. 12.15.11-12.15.11. New Jersey: John Wiley & Sons, Inc.

Eichten, A. E., Hyun, W. C. and Coussens, L. M. (2007). Distinctive features of angiogenesis and lymphangiogenesis determine their functionality during de novo tumor development. *Cancer Res.* **67**, 5211-5220.

Feng, D., Nagy, J. A., Hipp, J., Pyne, K., Dvorak, H. F. and Dvorak, A. M. (1997). Reinterpretation of endothelial cell gaps induced by vasoactive mediators in guinea-pig, mouse and rat: many are transcellular pores. *J. Physiol.* **504**, 747-761.

Feng, D., Nagy, J. A., Dvorak, H. F. and Dvorak, A. M. (2002). Ultrastructural studies define soluble macromolecular, particulate, and cellular transendothelial cell pathways in venules, lymphatic vessels, and tumor-associated microvessels in man and animals. *Microsc. Res. Tech.* **57**, 289-326.

Gade, T. P., Buchanan, I. M., Motley, M. W., Mazaheri, Y., Spees, W. M. and Koutcher, J. A. (2009). Imaging intratumoral convection: pressure-dependent enhancement in chemotherapeutic delivery to solid tumors. *Clin. Cancer Res.* **15**, 247-255.

Galardy, R. E., Grobelny, D., Foellmer, H. G. and Fernandez, L. A. (1994). Inhibition of angiogenesis by the matrix metalloprotease inhibitor N-[2R-2-(hydroxamidocarbonymethyl)-4-methylpentanoyl)]-L-tryptophan methylamide. *Cancer Res.* **54**, 4715-4718.

Gleizes, P. E. and Rifkin, D. B. (1999). Activation of latent TGF-beta. A required mechanism for vascular integrity. *Pathol. Biol. (Paris)* **47**, 322-329.

Guy, C. T., Cardiff, R. D. and Muller, W. J. (1992). Induction of mammary tumors by expression of polyomavirus middle T oncogene: a transgenic mouse model for metastatic disease. *Mol. Cell. Biol.* **12**, 954-961.

Haas, T. L., Stitelman, D., Davis, S. J., Apte, S. S. and Madri, J. A. (1999). Egr-1 mediates extracellular matrix-driven transcription of membrane type 1 matrix metalloproteinase in endothelium. *J. Biol. Chem.* **274**, 22679-22685.

Hashizume, H., Baluk, P., Morikawa, S., McLean, J. W., Thurston, G., Roberge, S., Jain, R. K. and McDonald, D. M. (2000). Openings between defective endothelial cells explain tumor vessel leakiness. *Am. J. Pathol.* **156**, 1363-1380.

Heldin, C. H., Rubin, K., Pietras, K. and Ostman, A. (2004). High interstitial fluid pressure-an obstacle in cancer therapy. *Nat. Rev. Cancer* **4**, 806-813.

Herron, G. S., Werb, Z., Dwyer, K. and Banda, M. J. (1986a). Secretion of metalloproteinases by stimulated capillary endothelial cells. I. Production of procollagenase and prostromelysin exceeds expression of proteolytic activity. *J. Biol. Chem.* **261**, 2810-2813.

Herron, G. S., Banda, M. J., Clark, E. J., Gavrilovic, J. and Werb, Z. (1986b). Secretion of metalloproteinases by stimulated capillary endothelial cells. II. Expression of collagenase and stromelysin activities is regulated by endogenous inhibitors. *J. Biol. Chem.* **261**, 2814-2818.

Hirschi, K. K., Rohovsky, S. A. and D'Amore, P. A. (1998). PDGF, TGF-beta, and heterotypic cell-cell interactions mediate endothelial cell-induced recruitment of 10T1/2 cells and their differentiation to a smooth muscle fate. *J. Cell Biol.* **141**, 805-814.

Inoue, H., Asaka, T., Nagata, N. and Koshihara, Y. (1997). Mechanism of mustard oil-induced skin inflammation in mice. *Eur. J. Pharmacol.* **333**, 231-240.

Ishida, W., Mori, Y., Lakos, G., Sun, L., Shan, F., Bowes, S., Josiah, S., Lee, W. C., Singh, J., Ling, L. E. et al. (2006). Intracellular TGF-beta receptor blockade abrogates Smad-dependent fibroblast activation in vitro and in vivo. *J. Invest. Dermatol.* **126**, 1733-1744.

Itoh, T., Ikeda, T., Gomi, H., Nakao, S., Suzuki, T. and Itohara, S. (1997). Unaltered secretion of beta-amyloid precursor protein in gelatinase A (matrix metalloproteinase 2)-deficient mice. *J. Biol. Chem.* **272**, 22389-22392.

Jacob, M. P., Badier-Commander, C., Fontaine, V., Benazzoug, Y., Feldman, L. and Michel, J. B. (2001). Extracellular matrix remodeling in the vascular wall. *Pathol. Biol. (Paris)* **49**, 326-332.

Kano, M. R., Bae, Y., Iwata, C., Morishita, Y., Yashiro, M., Oka, M., Fujii, T., Komuro, A., Kiyono, K., Kaminishi, M. et al. (2007). Improvement of cancer-targeting therapy, using nanocarriers for intractable solid tumors by inhibition of TGF-beta signaling. *Proc. Natl. Acad. Sci. USA* **104**, 3460-3465.

Lammerts, E., Roswall, P., Sundberg, C., Gotwals, P. J., Koteliansky, V. E., Reed, R. K., Heldin, N. E. and Rubin, K. (2002). Interference with TGF-beta1 and -beta3 in tumor stroma lowers tumor interstitial fluid pressure independently of growth in experimental carcinoma. *Int. J. Cancer* **102**, 453-462.

Lehti, K., Allen, E., Birkedal-Hansen, H., Holmbeck, K., Miyake, Y., Chun, T. H. and Weiss, S. J. (2005). An MT1-MMP-PDGF receptor-beta axis regulates mural cell investment of the microvasculature. *Genes Dev.* **19**, 979-991.

Liu, X., Wu, H., Byrne, M., Jeffrey, J., Krane, S. and Jaenisch, R. (1995). A targeted mutation at the known collagenase cleavage site in mouse type I collagen impairs tissue remodeling. *J. Cell Biol.* **130**, 227-237.

Loeffler, M., Kruger, J. A., Niethammer, A. G. and Reisfeld, R. A. (2006). Targeting tumor-associated fibroblasts improves cancer chemotherapy by increasing intratumoral drug uptake. *J. Clin. Invest.* **116**, 1955-1962.

Lu, S. L., Reh, D., Li, A. G., Woods, J., Corless, C. L., Kulesz-Martin, M. and Wang, X. J. (2004). Overexpression of transforming growth factor beta1 in head and neck epithelia results in inflammation, angiogenesis, and epithelial hyperproliferation. *Cancer Res.* **64**, 4405-4410.

Madri, J. A., Bell, L. and Merwin, J. R. (1992). Modulation of vascular cell behavior by transforming growth factors beta. *Mol. Reprod. Dev.* **32**, 121-126.

Maniatis, T., Fritsch, E. F. and Sambrook, J. (1982). *Molecular cloning: A laboratory manual.* Cold Spring Harbor: Cold Spring Harbor Laboratory Press.

McDonald, D. M. and Baluk, P. (2002). Significance of blood vessel leakiness in cancer. *Cancer Res.* **62**, 5381-5385.

McKee, T. D., Pluen, A., Boucher, Y., Ramanujan, S., Unemori, E., Seed, B. and Jain, R. K. (2001). Relaxin increases the transport of large molecules in high collagen content tumors. *Proc. Am. Assoc. Cancer Res.* **42**, 30.

McKee, T. D., Grandi, P., Mok, W., Alexandrakis, G., Insin, N., Zimmer, J. P., Bawendi, M. G., Boucher, Y., Breakefield, X. O. and Jain, R. K. (2006). Degradation of fibrillar collagen in a human melanoma xenograft improves the efficacy of an oncolytic herpes simplex virus vector. *Cancer Res.* **66**, 2509-2513.

Mehta, D. and Malik, A. B. (2006). Signaling mechanisms regulating endothelial permeability. *Physiol. Rev.* **86**, 279-367.

Miles, A. A. and Miles, E. M. (1952). Vascular reactions to histamine, histamine-liberator and leukotaxine in the skin of guinea pigs. *J. Physiol.* **118**, 228-257.

Miller, E. J. and Rhodes, R. K. (1982). Preparation and characterization of the different types of collagen. *Methods Enzymol.* **82**, 33-64.

Minchinton, A. I. and Tannock, I. F. (2006). Drug penetration in solid tumours. *Nat. Rev. Cancer* **6**, 583-592.

Mott, J. D. and Werb, Z. (2004). Regulation of matrix biology by matrix metalloproteinases. *Curr. Opin. Cell Biol.* **16**, 558-564.

Mu, D., Cambier, S., Fjellbirkeland, L., Baron, J. L., Munger, J. S., Kawakatsu, H., Sheppard, D., Broaddus, V. C. and Nishimura, S. L. (2002). The integrin alpha(v)beta8 mediates epithelial homeostasis through MT1-MMP-dependent activation of TGF-beta1. *J. Cell Biol.* **157**, 493-507.

Neptune, E. R., Frischmeyer, P. A., Arking, D. E., Myers, L., Bunton, T. E., Gayraud, B., Ramirez, F., Sakai, L. Y. and Dietz, H. C. (2003). Dysregulation of TGF-beta activation contributes to pathogenesis in Marfan syndrome. *Nat. Genet.* **33**, 407-411.

Overall, C. M. (2001). Matrix metalloproteinase substrate binding domains, modules and exosites. Overview and experimental strategies. *Methods Mol. Biol.* **151**, 79-120.

Padua, D., Zhang, X. H., Wang, Q., Nadal, C., Gerald, W. L., Gomis, R. R. and Massague, J. (2008). TGFbeta primes breast tumors for lung metastasis seeding through angiopoietin-like 4. *Cell* **133**, 66-77.

Page, R. C. and Schroeder, H. E. (1982). Periodontitiis in humans. In *Periodontitia in Man and Other Animals: A Comparative Review*, pp. 5-57. Basel, Switzerland: Karger.

Page-McCaw, A., Ewald, A. J. and Werb, Z. (2007). Matrix metalloproteinases and the regulation of tissue remodelling. *Nat. Rev. Mol. Cell Biol.* **8**, 221-233.

Parikh, S. M., Mammoto, T., Schultz, A., Yuan, H. T., Christiani, D., Karumanchi, S. A. and Sukhatme, V. P. (2006). Excess circulating angiopoietin-2 may contribute to pulmonary vascular leak in sepsis in humans. *PLoS Med.* **3**, e46.

Park, S. O., Lee, Y. J., Seki, T., Hong, K. H., Fliess, N., Jiang, Z., Park, A., Wu, X., Kaartinen, V., Roman, B. L. et al. (2008). ALK5- and TGFBR2-independent role of ALK1 in the pathogenesis of hereditary hemorrhagic telangiectasia type 2. *Blood* **111**, 633-642.

Pepper, M. S. (1997). Transforming growth factor-beta: vasculogenesis, angiogenesis, and vessel wall integrity. *Cytokine Growth Factor Rev.* **8**, 21-43.

Pittet, J. F., Griffiths, M. J., Geiser, T., Kaminski, N., Dalton, S. L., Huang, X., Brown, L. A., Gotwals, P. J., Koteliansky, V. E., Matthay, M. A. et al. (2001). TGF-beta is a critical mediator of acute lung injury. *J. Clin. Invest.* **107**, 1537-1544.

Pluen, A., Boucher, Y., Ramanujan, S., McKee, T. D., Gohongi, T., di Tomaso, E., Brown, E. B., Izumi, Y., Campbell, R. B., Berk, D. A. et al. (2001). Role of tumor-host interactions in interstitial diffusion of macromolecules: cranial vs. subcutaneous tumors. *Proc. Natl. Acad. Sci. USA* **98**, 4628-4633.

Predescu, D., Predescu, S. and Malik, A. B. (2002). Transport of nitrated albumin across continuous vascular endothelium. *Proc. Natl. Acad. Sci. USA* **99**, 13932-13937.

Ronaldson, P. T., Demarco, K. M., Sanchez-Covarrubias, L., Solinsky, C. M. and Davis, T. P. (2009). Transforming growth factor-beta signaling alters substrate permeability and tight junction protein expression at the blood-brain barrier during inflammatory pain. *J. Cereb. Blood Flow Metab.* **29**, 1084-1098.

Roviezzo, F., Tsigkos, S., Kotanidou, A., Bucci, M., Brancaleone, V., Cirino, G. and Papapetropoulos, A. (2005). Angiopoietin-2 causes inflammation in vivo by promoting vascular leakage. *J. Pharmacol. Exp. Ther.* **314**, 738-744.

Sato, Y. (1995). Activation of latent TGF-beta at the vascular wall-roles of endothelial cells and mural pericytes or smooth muscle cells. *J. Atheroscler. Thromb.* **2**, 24-29.

Seki, T., Yun, J. and Oh, S. P. (2003). Arterial endothelium-specific activin receptor-like kinase 1 expression suggests its role in arterialization and vascular remodeling. *Circ. Res.* **93**, 682-689.

Seki, T., Hong, K. H. and Oh, S. P. (2006). Nonoverlapping expression patterns of ALK1 and ALK5 reveal distinct roles of each receptor in vascular development. *Lab. Invest.* **86**, 116-129.

Sounni, N. E., Devy, L., Hajitou, A., Frankenne, F., Munaut, C., Gilles, C., Deroanne, C., Thompson, E. W., Foidart, J. M. and Noel, A. (2002). MT1-MMP expression promotes tumor growth and angiogenesis through an up-regulation of vascular endothelial growth factor expression. *FASEB J.* **16**, 555-564.

Stickens, D., Behonick, D. J., Ortega, N., Heyer, B., Hartenstein, B., Yu, Y., Fosang, A. J., Schorpp-Kistner, M., Angel, P. and Werb, Z. (2004). Altered endochondral bone development in matrix metalloproteinase 13-deficient mice. *Development* **131**, 5883-5895.

Su, G., Hodnett, M., Wu, N., Atakilit, A., Kosinski, C., Godzich, M., Huang, X. Z., Kim, J. K., Frank, J. A., Matthay, M. A. et al. (2007). Integrin alphavbeta5 regulates lung vascular permeability and pulmonary endothelial barrier function. *Am. J. Respir. Cell Mol. Biol.* **36**, 377-386.

Susic, D. (2007). Cross-link breakers as a new therapeutic approach to cardiovascular disease. *Biochem. Soc. Trans.* **35**, 853-856.

Tam, E. M., Wu, Y. I., Butler, G. S., Stack, M. S. and Overall, C. M. (2002). Collagen binding properties of the membrane type-1 matrix metalloproteinase (MT1-MMP) hemopexin C domain. The ectodomain of the 44-kDa autocatalytic product of MT1-MMP inhibits cell invasion by disrupting native type I collagen cleavage. *J. Biol. Chem.* **277**, 39005-39014.

Tam, E. M., Morrison, C. J., Wu, Y., Stack, M. S. and Overall, C. M. (2004). Membrane protease proteomics: Isotope-coded affinity tag MS identification of undescribed MT1-matrix metalloproteinase substrates. *PNAS* **101**, 6917-6922.

Thurston, G., Baluk, P., Hirata, A. and McDonald, D. M. (1996). Permeability-related changes revealed at endothelial cell borders in inflamed venules by lectin binding. *Am. J. Physiol.* **271**, 2547-2562.

Thurston, G., Murphy, T. J., Baluk, P., Lindsey, J. R. and McDonald, D. M. (1998). Angiogenesis in mice with chronic airway inflammation: strain-dependent differences. *Am. J. Pathol.* **153**, 1099-1112.

Tuxhorn, J. A., McAlhany, S. J., Yang, F., Dang, T. D. and Rowley, D. R. (2002). Inhibition of transforming growth factor-beta activity decreases angiogenesis in a human prostate cancer-reactive stroma xenograft model. *Cancer Res.* **62**, 6021-6025.

Verbeek, M. M., Otte-Holler, I., Wesseling, P., Ruiter, D. J. and de Waal, R. M. (1994). Induction of alpha-smooth muscle actin expression in cultured human brain pericytes by transforming growth factor-beta 1. *Am. J. Pathol.* **144**, 372-382.

Vinals, F. and Pouyssegur, J. (2001). Transforming growth factor beta1 (TGF-beta1) promotes endothelial cell survival during in vitro angiogenesis via an autocrine mechanism implicating TGF-alpha signaling. *Mol. Cell. Biol.* **21**, 7218-7230.

Wang, M., Zhao, D., Spinetti, G., Zhang, J., Jiang, L. Q., Pintus, G., Monticone, R. and Lakatta, E. G. (2006). Matrix metalloproteinase 2 activation of transforming growth factor-beta1 (TGF-beta1) and TGF-beta1-type II receptor signaling within the aged arterial wall. *Arterioscler. Thromb. Vasc. Biol.* **26**, 1503-1509.

Werb, Z. (1997). ECM and cell surface proteolysis: regulating cellular ecology. *Cell* **91**, 439-442.

Woessner, J. F. (1961). The determination of hydroxyproline in tissue and protein samples containing small portions of this imino acid. *Arch. Biochem. Biophys* **93**, 440-447.

Yamamoto, T., Takagawa, S., Katayama, I. and Nishioka, K. (1999). Anti-sclerotic effect of transforming growth factor-beta antibody in a mouse model of bleomycin-induced scleroderma. *Clin. Immunol.* **92**, 6-13.

Yan, Q. and Sage, E. H. (1998). Transforming growth factor-beta1 induces apoptotic cell death in cultured retinal endothelial cells but not pericytes: association with decreased expression of p21waf1/cip1. *J. Cell Biochem.* **70**, 70-83.

Yu, Q. and Stamenkovic, I. (2000). Cell surface-localized matrix metalloproteinase-9 proteolytically activates TGF-beta and promotes tumor invasion and angiogenesis. *Genes Dev.* **14**, 163-176.

Zheng, T., Zhu, Z., Wang, Z., Homer, R. J., Ma, B., Riese, R. J., Jr, Chapman, H. A., Jr, Shapiro, S. D. and Elias, J. A. (2000). Inducible targeting of IL-13 to the adult lung causes matrix metalloproteinase- and cathepsin-dependent emphysema. *J. Clin. Invest.* **106**, 1081-1093.

Zhou, Z., Apte, S. S., Soininen, R., Cao, R., Baaklini, G. Y., Rauser, R. W., Wang, J., Cao, Y. and Tryggvason, K. (2000). Impaired endochondral ossification and angiogenesis in mice deficient in membrane-type matrix metalloproteinase I. *Proc. Natl. Acad. Sci. USA* **97**, 4052-4057.

Disease Models & Mechanisms • DMM